Insights into CO/Styrene Copolymerization by Using Pd^{II} Catalysts Containing Modular Pyridine–Imidazoline Ligands

Amaia Bastero,*[a] Carmen Claver,*[a] Aurora Ruiz,[a] Sergio Castillón,[b] Elias Daura,[a] Carles Bo,[a] and Ennio Zangrando[c]

Abstract: Continuing our studies into the effect that N–N′ ligands have on CO/styrene copolymerization, we prepared new C_1-symmetrical pyridine–imidazoline ligands with 4′,5′-*cis* stereochemistry in the imidazoline ring (**5**) and 4′,5′-*trans* stereochemistry (**6**–**10**) and compared them with our previously reported ligands (**1**–**4**). Their coordination to neutral methylpalladium(II) (**5a**–**10a**) and cationic complexes (**5b**–**10b**), investigated in solution by NMR spectroscopy, indicates that both the electronic and steric properties of the imidazolines determine the stereochemistry of the palladium complexes. The crystal structures of two neutral palladium precursors $[Pd(Me)_{2-n}Cl_n(N{-}N')]$ ($n=1$ for **8a**; $n=2$ for **9a′**) show that the Pd–N coordination distances and the geometrical distortions in the imidazoline ring depend on the electronic nature of the substituents in the imidazoline fragment. Density functional calculations performed on selected neutral and cationic palladium complexes compare well with NMR and X-ray data. The calculations also account for the formation of only one or two stereoisomers of the cationic complexes. The performance of the cationic complexes as catalyst precursors in CO/4-*tert*-butylstyrene copolymerization under mild pressures and temperatures was analyzed in terms of the productivity and degree of stereoregularity of the polyketones obtained. Insertion of CO into the Pd–Me bond, which was monitored by multinuclear NMR spectroscopy, shows that the N ligand influences the stereochemistry of the acyl species formed.

Keywords: copolymerization · density functional calculations · ligand design · N ligands · palladium

Introduction

Late-transition-metal complexes can be used as polymerization catalysts to access polymeric structures containing polar monomers.[1] In particular, metal-catalyzed copolymerization of carbon monoxide with alkenes provides greater control over the polymer properties than radical polymerization, and makes it possible to synthesise alternating polyketones. The low cost of the starting materials and the material properties of the products also make it an attractive reaction.[2–4] Several mechanistic studies have been performed with well-defined single-site catalysts.[5–10] However, the search for chiral ligands that lead to the formation of regular microstructures is still an interesting topic.[11]

Palladium catalysts bearing nitrogen-donor ligands have proved to be effective for CO/styrene copolymerization,[2,12] unlike palladium–diphosphane catalysts, which generally form oligomers.[13] In most cases bidentate N ligands[14–21] and, to a lesser extent, hemilabile P,N ligands have been used successfully.[7,21] The common feature in all these ligands is the sp^2 character of the coordinating N atom. Oxazolines are effective ligands in several metal-catalyzed homogeneous reactions[22] including CO/styrene copolymerization.[15,16,21] We believed that imidazolines, which are structurally analogous but which have different electronic properties,[23–27] could be good alternatives. Therefore, we developed racemic 1-substituted (*R*,*S*)-4,5-dihydro-4,5-diphenyl-2-(2-pyridyl)imidazoles **1**–**4** with 4′,5′-*cis* stereochemistry in the imidazoline moiety, which have the advantage that the substituent in the aminic nitrogen atom N_1 can be easily modified to lead to a series of chiral ligands (Figure 1).[28] This substitution makes it possible to fine tune the electronic properties of the imidazoline ring over a wide

[a] Dr. A. Bastero, Prof. Dr. C. Claver, Dr. A. Ruiz, E. Daura, Dr. C. Bo
Departament de Química Física i Inorgànica
Universitat Rovira i Virgili
Pl. Imperial Tàrraco 1, 43005 Tarragona (Spain)
Fax: (+34) 977-559-563
E-mail: claver@quimica.urv.es

[b] Prof. Dr. S. Castillón
Departament de Química Orgànica i Química Analítica
Universitat Rovira i Virgili
Pl. Imperial Tàrraco 1, 43005 Tarragona (Spain)

[c] Dr. E. Zangrando
Dipartimento di Scienze Chimiche
Università degli Studi di Trieste
Via Licio Giorgieri 1, 34127 Trieste (Italy)

Supporting information for this article is available on the WWW under http://www.chemeurj.org/ or from the author.

 DOI: 10.1002/chem.200306051

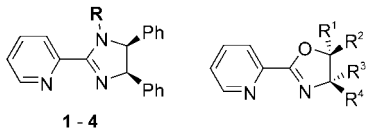

Figure 1. Pyridine–imidazolines **1**–**4** in comparison with the general structure of pyridine-oxazolines.

range without changing the chiral environment around the donor N atom.

Modifying the electronic properties of palladium catalysts by using different ligands may lead to variations not only in the activity, but also in the selectivity.[29] The use of palladium(II) catalysts containing chiral C_1-symmetrical pyridine-oxazoline ligands in CO/styrene copolymerization leads to syndiotactic polyketones.[15,21] This is because the site-selective coordination of the styrene *cis* to the pyridine moiety means that the stereocontrol of the reaction is provided by chain-end control and not by the chiral ligand (enantiosite control) (Figure 2).[21] So it seems that to increase the co-

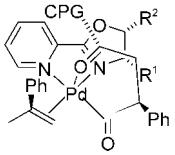

Figure 2. Model proposed by Consiglio et al. for styrene insertion to give predominantly syndiotactic copolymer. GPC = growing polymer chain.

polymer content of *l* diads with our pyridine–imidazolines, styrene must be selectively coordinated *cis* to the chiral imidazoline. For this reason we decided to take into account both steric and electronic factors in ligand design.

We have now synthesized 1-substituted (*R*,*R*)-4,5-dihydro-4,5-diphenyl-2-(2-pyridyl)imidazoles **6**–**10** with 4′,5′-*trans* stereochemistry in the imidazoline (Scheme 1). The coordination of these ligands to neutral and cationic palladium complexes was investigated in solution, and their structures were compared by X-ray diffraction and DFT calculations. The activity of the cationic palladium(II) complexes in CO/4-*tert*-butylstyrene copolymerization was studied and compared with our data on pyridine–imidazolines with 4′-5′-*cis* stereochemistry.[28] Since site-selective coordination is crucial for stereocontrol of the reaction, we analyzed the reactivity of the complexes towards CO by NMR spectroscopy, that is, monitoring the first step of the catalytic cycle.

Results and Discussion

Synthesis and characterization of ligands: We first prepared pyridine–imidazoline ligands **1**–**4**, whose phenyl rings in the imidazoline moiety are in mutually *cis* positions (Scheme 1). We observed that modifying the R substituent in the imidazoline ring influenced the properties of the binding N atom. This led to palladium complexes with different stereochemistries, which catalyzed the synthesis of polyketones with different degrees of stereoregularity.[28] To try to promote the coordination of styrene *cis* to the imidazoline, we increased the steric hindrance near the pyridine N atom and simultaneously decreased the basicity of the pyridine ring by synthesising racemic (*R*,*S*)-4,5-dihydro-4,5-diphenyl-2-(6-cyanopyridyl)imidazole (**5**; Scheme 1). The product is obtained in a low yield (20%) since the bis-anellation product is also formed.[30] Since it was recently reported that in CO/ethene copolymerization palladium catalysts containing (*R*,*S*)- or (*S*,*R*)-*meso*-diphosphanes behave differently to those bearing the ligands with *R*,*R* or *S*,*S* configuration (Figure 3),[31,32] we tested the effect of varying the stereochemistry of our imidazolines by preparing ligands **6**–**10**.

Enantiomerically pure (*R*,*R*)-pyridine–imidazoline **6** was prepared in quantitative yield by reaction of the corresponding diamine and 2-cyanopyridine, similar to **1** (Scheme 1). Reaction of **6** with different electrophiles (benzyl bromide, methyl iodide, *p*-toluenesulfonyl chloride, and trifluoromethylsulphonyl anhydride) in the presence of a base gave the substituted (*R*,*R*)-pyridine–imidazolines **7**–**10** (Scheme 1). The ^{1}H NMR spectra of these ligands show the characteristic two doublets corresponding to $H^{4'}$ and $H^{5'}$ of the imidazoline moiety (see Scheme 1 for numbering). In the case of **6**, the two doublets become a singlet at 5 ppm due to tautomeric equilibrium. A comparison of the coupling constants of these two protons in ligands **1**–**10** shows that the nature of the R substituent has an effect on the coupling constant $^3J(4',5')$,[33]

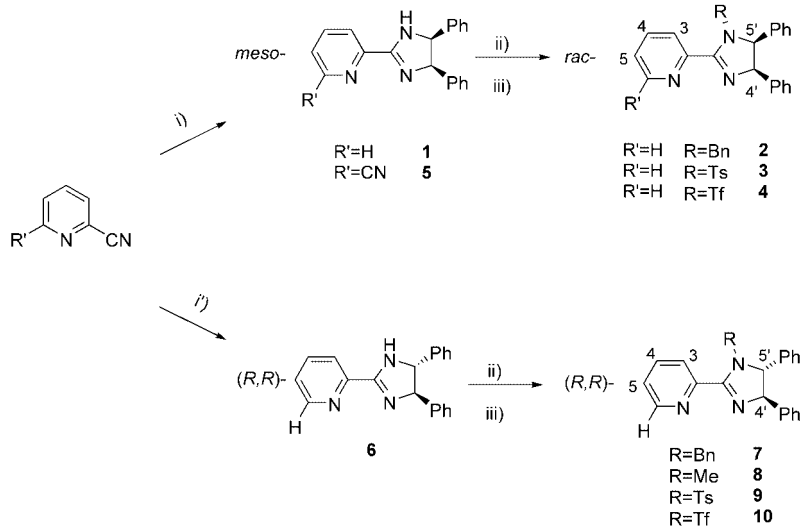

Scheme 1. Synthesis of ligands **1**–**10** showing numbering scheme. i) *meso*-(1*R*,2*S*)-1,2-Diphenylethylenediamine. i′) (1*R*,2*R*)-1,2-diphenylethylenediamine; ii) 4-dimethylaminopyridine for **3**, **4**, **9**, **10**; NaH for **2**, **7**, **8**; iii) BnBr for **2**, **7**; TsCl for **3**, **9**; MeI for **8**; Tf_2O for **10**.

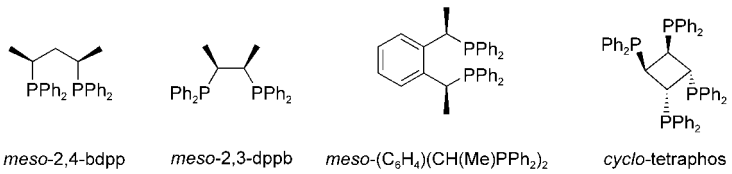

Figure 3. *meso*-Diphosphanes used as ligands in CO/ethene copolymerization.

which decreases for the electron-withdrawing, bulky *p*-toluenesulfonyl (Ts) and trifluoromethylsulfonyl (Tf) groups (Table 1). It is worth noting that for enantiomerically pure (*R*,*R*)-ligands **7**–**10** these variations are more pronounced than for racemic (*R*,*S*)-ligands **2**–**4**.[28]

Table 1. Selected ^{1}H NMR data for ligands **1**–**10** in $CDCl_3$ at room temperature.

Ligand	R	$H^{4'}$, $H^{5'}$	$^3J_{4'-5'}$ [Hz]
1	H	5.51	–
2	Bn	5.44, 4.92	11.6
3	Ts	5.93, 5.80	10
4	Tf	5.98, 5.92	8.7
5	H	5.58	–
6	H	5.0	–
7	Bn	5.0, 4.42	9.2
8	Me	4.86, 4.25	10.5
9	Ts	5.36, 5.17	4.8
10	Tf	5.45, 5.37	3.8

Synthesis and characterization of and DFT calculations of neutral methylpalladium(II) complexes: Similar to what was observed for ligands **1**–**4**,[34] the reaction of ligands **5**–**10** with [PdClMe(cod)] (cod = 1,5-cyclooctadiene) in toluene at room temperature led to precipitation of neutral complexes **5a**–**10a** (Scheme 2).

Characterization of these complexes in solution by multinuclear NMR spectroscopy showed the presence of only one isomer. For complexes **6a**–**10a** in the aromatic region of the ^{1}H NMR spectra, the signal for H^6 (see Scheme 1) is considerably shifted downfield with respect to that in the free ligand ($\Delta\delta = 0.52$ ppm). This indicates that H^6 is subject to the anisotropic effect of the neighboring chloro ligand.[35] NOE experiments show the interaction between the PdMe group and $H^{4'}$ of the imidazoline ring, which confirms that all neutral complexes **5a**–**10a** are *cis* isomers (where *cis* and *trans* indicate the stereochemical relationship between the methyl group and the imidazoline ring). In the spectra of complexes **6a**–**9a** the methyl group bonded to palladium appears as an upfield-shifted singlet (average shift: 0.47 ppm; Table 2). Since a methyl group σ-bonded to palladium normally appears at around 1 ppm,[36] the presence of this signal at lower frequencies may be due to the unusual proximity between the methyl group and the phenyl ring in the 4′-position in these complexes.

The *cis* stereochemistry was also observed in the solid state for complex **8a**. Single crystals suitable for X-ray analysis were obtained for this neutral complex, which contains a ligand substituted with an electron-donating group (R = Me; Figure 4). Efforts to obtain single crystals of complex **9a**, with a ligand bearing an electron-withdrawing group (R = Ts), resulted in isolation of [$PdCl_2$(**9**)] (**9a′**; Figure 5).[37]

To complete the study on the coordination of the (*R*,*R*)-pyridine–imidazolines to palladium, DFT calculations were performed for complexes **6a** and **10a**. Table 3 shows a selection of measured bond lengths and angles of the molecular structures for the neutral complexes **8a** and **9a′**, and calculated values for **6a** and **10a**.

The Pd–N(py) distances are longer than those involving the iminic N atom of the imidazoline N atom N2 (Table 3). The Pd–N1 distance observed in **8a** is particularly long (2.121(6) Å), because of the *trans* influence exerted by the methyl group coordinated to palladium (Figure 4). On the

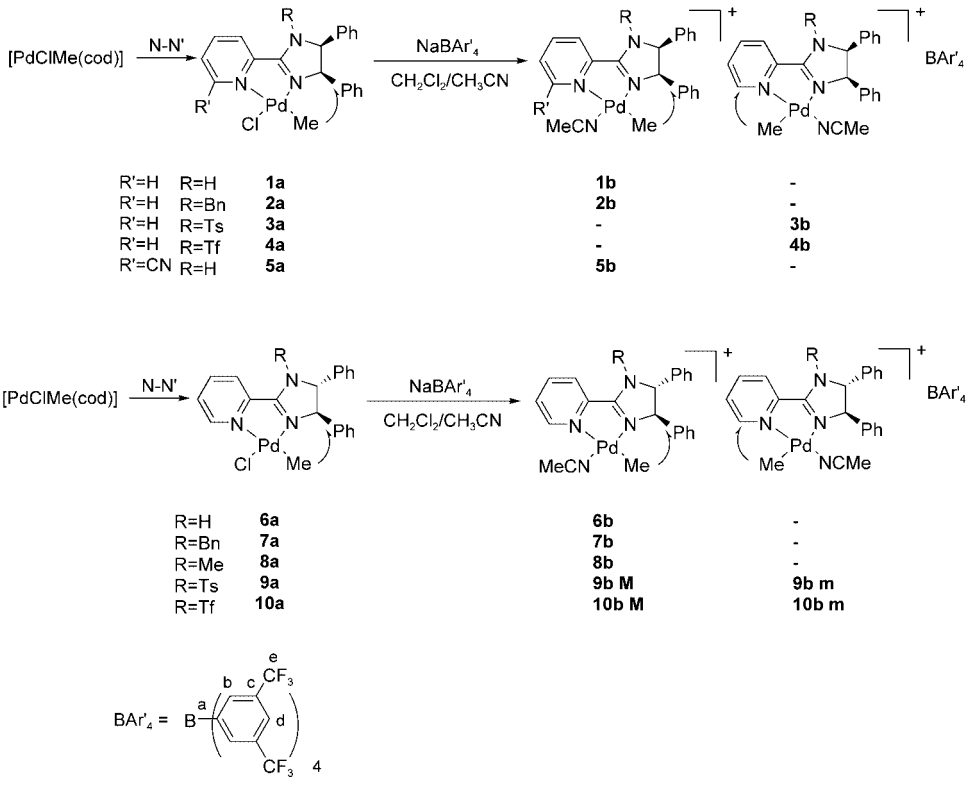

Scheme 2. Synthesis of **1a**–**10a** and **1b**–**10b**. The numbering Scheme of Ar'_4B^- is included.

Table 2. Selected ^{1}H NMR data for complexes **5a**–**10a** and **5b**–**10b** in $CDCl_3$ at room temperature.[a]

Compound	H^6	PdMe	PdNCMe
5a[b]	–	0.72	–
6a	8.82 (d)	0.34	–
7a	9.26 (d)	0.52	–
8a	9.28 (d)	0.48	–
9a	9.24 (d)	0.55	–
10a	9.29 (d)	0.75	–
5b	–	0.90	2.33
6b	8.34 (d)	0.56	2.30
7b	8.38 (d)	0.54	2.28
8b	8.38 (d)	0.48	2.30
9b[c]	M: 8.35 (dd)	0.57	2.20
	m: 8.50 (d)	0.97	1.61
10b[c]	M: 8.38 (d)	0.74	2.26
	m: 8.52 (d)	1.07	1.73

[a] The signals are singlets unless otherwise stated. Coupling constants are omitted for clarity. [b] In $(CD_3)_2(CO)$. [c] M: major isomer; m: minor isomer.

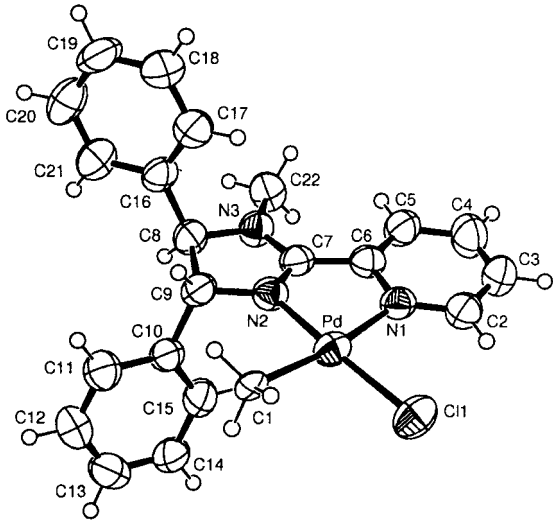

Figure 4. ORTEP plot (40% probability thermal ellipsoids) of the molecular structure of **8a**.

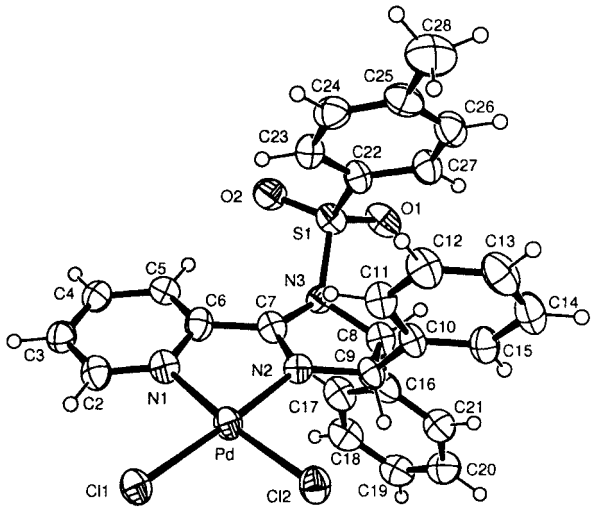

Figure 5. ORTEP plot (40% probability thermal ellipsoids) of the molecular structure of **9a′**.

other hand, the Pd–N2 bond lengths of 2.021(5) Å in **8a** and 2.013(5) Å in **9a′** seem to be slightly influenced by the different electronic properties of the R group in the imidazoline ring. The calculated values in Table 3 compare fairly well with the X-ray values. The Pd–Cl and Pd–C coordination distances fall in a range that has often been observed in other Pd^{II} complexes.[34,38] The chelating ligand, the small N1-C6-C7-N2 torsion angles of 5.2(8)° in **8a** and 2.1(9)° in **9a′** indicate negligible tilting between the rings. Similar torsion angles of 0.7° in **6a** and 8.0° in **10a** were found for the calculated complexes. However, the dihedral angle formed by the best-fit planes through the rings are significantly different: 2.6(4)° in **8a**, 3.0° in **6a**, 7.6° in **10a**, and 17.9(3)° in **9a′**. The large angle in **9a′** might be ascribed to a distortion in the imidazoline plane that favors intramolecular π stacking of the tosyl ring with the adjacent phenyl group (distance between centroids 3.747 Å; Figure 5). The electron-withdrawing tosyl group in **9a′** causes the N2–C7 and N3–C7 distances to be different (1.281(8) and 1.427(8) Å, respectively), while in **8a** (R = Me) these bond lengths are similar (1.293(9) and 1.330(8) Å). Correspondingly, the sum of the bond angles about the imidazoline N atom N3 is 360.0° in **8a** and 348.1° in **9a′**. This electronic effect is very well reproduced by the DFT calculations for complexes **6a** and **10a**.

In view of the large *trans* influence of the methyl group, it is expected to be *trans* to the less basic ring (pyridine in **5a**–

Table 3. Selected bond lengths [Å] and angles [°] for **8a**, **9a′**, **6a** and **10a**.

	8a X = C1	**9a′** X = Cl2	**6a**[a] X = C1	**10a**[a] X = C1
Pd–N1	2.121(6)	2.049(5)	2.168	2.149
Pd–N2	2.021(5)	2.013(5)	2.030	2.017
Pd–Cl1	2.303(2)	2.289(2)	2.301	2.292
Pd–X	2.181(4)	2.277(2)	2.033	2.040
N2–C7	1.293(9)	1.281(8)	1.307	1.308
N2–C9	1.462(8)	1.444(8)	1.474	1.467
N3–C7	1.330(8)	1.427(8)	1.382	1.431
N3–C8	1.467(9)	1.480(8)	1.488	1.509
N3–C22	1.477(9)	–	–	–
N3–S1	–	1.693(5)	–	1.686
N1-Pd-N2	78.4(2)	79.9(2)	77.5	76.5
N1-Pd-Cl1	96.00(16)	95.41(16)	96.1	97.1
N1-Pd-X	171.9(2)	172.57(15)	172.6	172.7
N2-Pd-Cl1	173.22(16)	175.15(14)	173.4	173.4
N2-Pd-X	94.5(2)	92.79(15)	95.3	97.2
Cl1-Pd-X	91.30(12)	91.81(6)	91.1	89.3
N3-S1-C22	–	108.2(3)	–	–
N1-C6-C7-N2	5.2(8)	2.1(9)	–0.7	8.0
C16-C8-C9-C10	125.8(6)	139.7(6)	134.7	114.8
dihedral angle py/im	2.6(4)	17.9(3)	3.0	7.6

[a] QM/MM calculations.

8a, and imidazoline in **9a** and **10a**). Because we were intrigued by the *cis* stereochemistry of all the complexes and wished to know whether an isomeric equilibrium—not detected by low-temperature NMR spectroscopy—was present, we performed DFT calculations of some representative examples. One reason for the *cis* stereochemistry observed for all the neutral complexes **1a**–**10a** was found to be the relative energy of the *cis* and *trans* isomers, calculated for complexes **1a**, **4a**, **6a**, **10a** (Table 4). The *cis* isomer was the most stable in all cases. Note that the relative stability of the *cis*/*trans* isomers depends on the electronic effect exerted by the R substituent. The relative stability decreases when the withdrawing character of R increases (**4a** and **10a** vs **1a** and **6a**). However, the stereochemistry of the imidazolines (*R*,*S* for complexes **1a**, **4a**; *R*,*R* for complexes **6a**, **10a**) was found to have no steric effect.

Table 4. Relative stabilities of *cis*/*trans* isomers of complexes **1a**/**6a** and **4a**/**10a** [energies in kJ mol^{-1}].

Stereoisomer	R = H		R = Tf	
	1a	**6a**	**4a**	**10a**
cis	0.0	0.0	0.0	0.0
trans	14.6	12.1	2.9	6.3

Synthesis and characterization and DFT calculations of cationic palladium(II) complexes: The neutral complexes were treated with $NaBAr'_4$ in the presence of acetonitrile to obtain the cationic complexes $[PdMe(NCMe)(N{-}N')]BAr'_4$ (**5b**–**10b**; Scheme 2). They were completely characterized in solution by NMR spectroscopy. The most significant signals are those related to H^6 for the ligand and to the Pd–Me and Pd–NCMe fragments (Table 2). For complexes **5b**–**8b**, which contain electron-donating substituents, one set of signals is evident at room temperature. All signals are shifted with respect to the free ligand, which indicates that coordination has taken place. For complexes **6b**–**8b**, the signals of the methyl and acetonitrile ligands coordinated to palladium appear as singlets between 0.48 and 0.56, and 2.28 and 2.30 ppm, respectively (Table 2). These shifts are indicative of *cis* stereoisomers.[34] In the case of **5b**, the Pd–Me signal is subject to the effect of the cyano-substituted pyridine ring in the *trans* position and appears further downfield (0.90 ppm). By irradiating the signal of the methyl group bound to palladium, an NOE interaction with $H^{4'}$ of the imidazoline ring became evident. For complexes **5b**–**8b**, this confirmed the presence of only one species in solution, whose Pd–Me bond is *cis* to the imidazoline ring (Scheme 2).

In contrast, **9b** and **10b** showed two sets of resonances in solution at room temperature, in both the aromatic and the aliphatic parts of the spectra (Table 2). COSY experiments together with selective irradiation of the aromatic signals confirmed the presence of *cis*/*trans* stereoisomers in ratios of 3:1 for **9b** and 2:1 for **10b**.

Although crystals suitable for structure determination were not obtained for the cationic complexes, the structural parameters for the *cis* and *trans* isomers of the cationic complexes **1b**, **4b**, **6b**, and **10b** (as representative examples) were determined by means of DFT calculations. No great differences were found between the molecular structures of the cationic complexes and those of the neutral complexes described above.[39] The most significant feature is found in the N2–C7 and N3–C7 bond lengths (see Figure 4 for numbering). Both bond lengths are sensitive to the R substituents, as was found for the neutral complexes. The values indicate that when R = H, the N2–C7 and N3–C7 distances are similar because of electronic delocalization through the amidine fragment (e.g., for *cis*-**1b**: 1.310 vs 1.306 Å, respectively). When R = Tf, the N2–C7 distance is shorter than the N3–C7 distance (e.g., for *cis*-**4b**: 1.306 vs 1.407 Å, respectively). The same effect can be observed in the case of **6b** and **10b**. However, these bond lengths are not as different in the cationic complexes as in the neutral complexes. Therefore, in the cationic complexes conjugation between the imine and amine moieties in the imidazoline moiety is more pronounced than in the neutral complexes. This is in agreement with the fact that the electrophilicity is expected to be higher for a cationic complex than for a neutral one.

The relative energy of the *cis*/*trans* isomers was also calculated for complexes **1b**, **4b**, **6b** and **10b** (Table 5). First, we observed that for the cationic complexes the difference in the relative energy of the stereoisomers is lower than that calculated for the neutral complexes (Table 4). The *cis* isomer was the most stable isomer for complexes **1b**, **6b**, and **10b**, while for **4b** the two isomers were almost degenerate in energy and the *trans* form was slightly more stable. Although these small energy differences may not be significant, we note that they are in good agreement with what we observed experimentally (see Scheme 2).

Table 5. Relative stabilities of complexes **1b**/**6b** and **4b**/**10b** [energies in kJ mol^{-1}].

Stereoisomer	R = H		R = Tf	
	1b	**6b**	**4b**	**10b**
cis	0.0	0.0	0.4	0.0
trans	8.8	5.0	0.0	2.5

To sum up, for the cationic complexes **1b**–**5b**, which bear the (*R*,*S*)-pyridine–imidazoline ligands (4′,5′-*cis* stereochemistry), the coordination of the Me group to palladium is determined by the electronic nature of the R substituents in the imidazoline. Consequently the methyl group is always *trans* to the less basic ring (pyridine for complexes **1b**, **2b**, **5b**, and imidazoline for **3b** and **4b**). However, complexes **6b**–**10b**, which bear the (*R*,*R*)-ligands (4′,5′-*trans* stereochemistry), are always present as *cis* stereoisomers (the single species for complexes **6b**–**8b**, and the major one in a mixture of isomers for **9b**, **10b**). Therefore, in the latter case, both the electronic nature and the stereochemistry of the ligand must be responsible for determining the stereochemistry.

These small energy differences between the calculated values for *cis*/*trans* isomers (Table 5) suggest that the two isomers are in equilibrium. The sharpness of the NMR signals seems to exclude the presence of an equilibrium,[40] so we considered that the stereochemistry of the complexes

should be determined during their formation. Although a full mechanistic study is beyond the scope of this paper, we attempted to locate possible intermediates along the reaction path to obtain some insight into the formation of the cationic palladium stereoisomers (Scheme 2). The first question that arises at this point is whether the mechanism that forms these cationic complexes is associative or dissociative. Several attempts to determine the geometry of a five-coordinate intermediate (associative path), either a square-based pyramid or trigonal bipyramid (see Scheme 3), failed and led to ligand dissociation. We therefore concluded that an associative mechanism is not plausible.

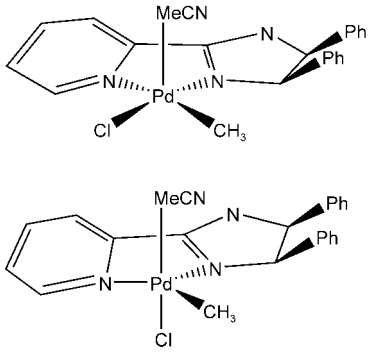

Scheme 3. Possible square-based pyramidal and trigonal-bipyramidal intermediates.

Hence, we considered dissociation of a ligand leading to a three-coordinate species prior to acetonitrile coordination. As was suggested in a recent study on similar pyridine–pyrazole ligands,[41] we considered a T-shaped intermediate corresponding to dissociation of the pyridine moiety (**A** in Figure 6). The energy required to form **A** from its neutral counterpart is calculated to be 83.6 kJ mol^{-1}, which is a reasonable value for a barrier. The subsequent coordination of acetonitrile provides different possibilities. To test some of them, we considered complexes **B** and **C** (Figure 6), which should involve ligand exchange (chloride by acetonitrile) in an axial direction, perpendicular to the former square-planar neutral complex. In both complexes we observed square-planar coordination, with the pyridine (**C**) or imidazoline (**B**) moiety in the axial position. The energy difference between **B** and **C** is large enough to suggest that pyridine dissociation is preferred. From complex **C**, the chloride ligand should dissociate, and then coordination of the pyridinic arm and reorganization leading to the square-planar complex should follow. We propose that such intermediates account for the structures obtained for the cationic complexes. The combination of the electronic effects exerted by these ligands with the steric hindrance that the phenyl rings of the imidazoline moiety may impose on acetonitrile coordination and on the reorganization step seems to be a plausible explanation for the formation of only one isomer or both isomers.

Synthesis and structure of cationic rhodium complexes 1c–4c and 1d–4d: To obtain more information about the basicities of pyridine–imidazoline ligands **1**–**4** (Scheme 1), we synthesised a series of bis-carbonyl rhodium complexes and measured their CO frequencies by IR spectroscopy. The reaction of ligands **1**–**4** with $[Rh(cod)_2]BF_4$ in dichloromethane resulted in the displacement of one molecule of 1,5-cyclooctadiene to afford the cationic complexes [Rh(cod)(N–N′)]BF_4 (**1c**–**4c**). The ^{1}H NMR spectra showed one set of signals for the N ligand, but various broad signals for the coordinated 1,5-cyclooctadiene (see Experimental Section). Considering the C_1 symmetry of the rhodium(I) cation, four signals are expected for the olefinic protons, although fluxionality may restrict the number of signals observed. Interestingly, the number of signals observed at room temperature for the olefinic protons depended on the substituent on the N ligand. Low-temperature NMR spectroscopy showed

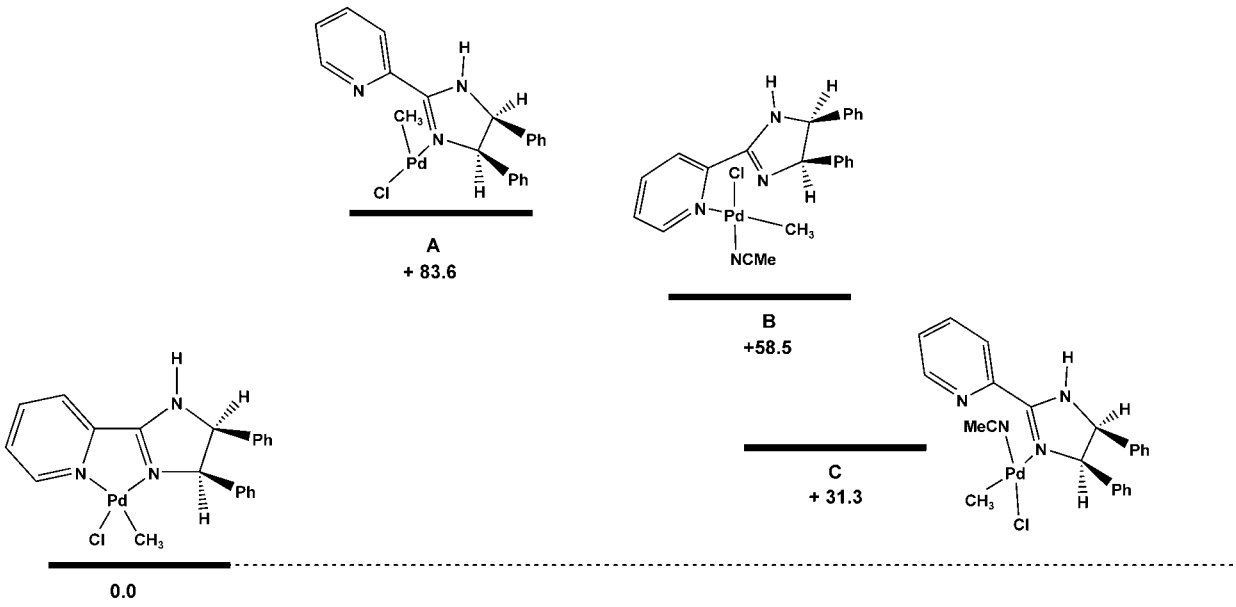

Figure 6. Selected intermediates for the dissociative pathway. [energies in kJ mol^{-1}].

the expected four signals for the four complexes. This gives further proof that modifying the remote substituent R tunes the electronic nature of the pyridine–imidazolines.

Suitable crystals for X-ray diffraction were obtained for complexes **2c** and **3c**. The X-ray structure shows the rhodium atom with the expected square-planar coordination by the N donors of the chelating pyridine–imidazoline ligand and the two double bonds of 1,5-cyclooctadiene. Figures 7 and 8 show perspective views of **2c** and **3c**, respectively. The

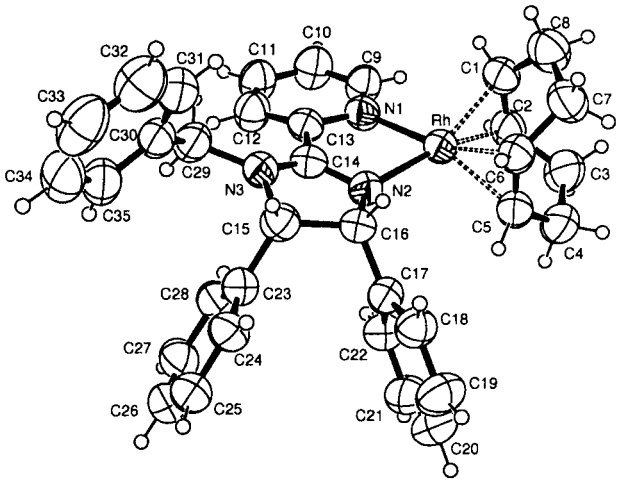

Figure 7. ORTEP plot (40% probability thermal ellipsoids) of the molecular structure of the cation of **2c**.

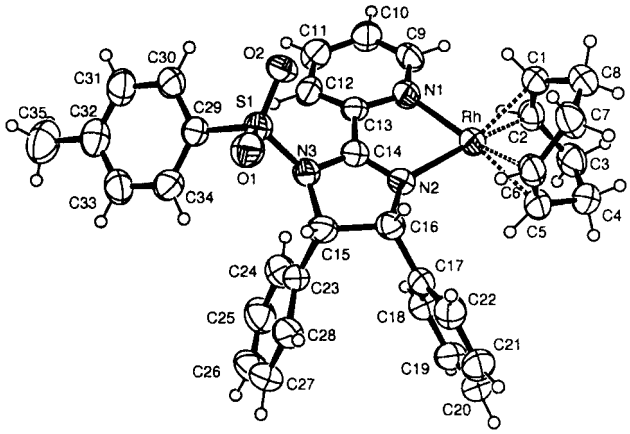

Figure 8. ORTEP plot (40% probability thermal ellipsoids) of the molecular structure of the cation of **3c**.

Rh–C bonds (Table 6), which lie in a wide range (2.124(8)–2.169(7) Å), and the alkene C–C bonds (av 1.38 Å) agree with those found in other Rh(cod) complexes.[42] Taking C1m and C5m as the midpoints of the alkene C=C bonds, the calculated distances *trans* to N2 and N1 are Rh–C1m 2.008 and 2.009 Å, and Rh–C5m 2.033 and 2.047 Å, for **2c** and **3c**, respectively. The coordination mean plane N1-N2-C1m-C5m forms an angle close to 88° with the plane calculated through the alkene C atoms.

In both complexes the Rh–N1(pyridine) bond length is slightly longer than the Rh–N2(imidazoline) bond length.

Table 6. Selected bond lengths [Å] and angles [°] for **2c** and **3c**.[a]

	2c	**3c**
Rh–N1	2.099(5)	2.112(6)
Rh–N2	2.078(5)	2.090(6)
Rh–C1	2.124(8)	2.125(7)
Rh–C2	2.139(7)	2.131(7)
Rh–C5	2.139(6)	2.169(7)
Rh–C6	2.147(6)	2.152(7)
Rh–C1m	2.008	2.009
Rh–C5m	2.033	2.047
N2–C14	1.324(7)	1.283(8)
N2–C16	1.484(7)	1.502(8)
N3–C14	1.336(8)	1.387(9)
N3–C15	1.483(8)	1.496(8)
N3–C29	1.480(8)	–
N3–S1	–	1.692(5)
C1–C2	1.393(10)	1.375(10)
C5–C6	1.378(10)	1.363(11)
N1-Rh-N2	78.2(2)	77.9(2)
C1m-Rh-C5m	87.41	87.32
N3-C29-C30	112.0(5)	–
N3-S1-C29	–	105.7(3)
N1-C13-C14-N2	−13.5(8)	−16.5(9)
C23-C15-C16-C17	−16.9(7)	−26.9(9)
C29-N3-C15-C23	62.8(7)	–
S1-N3-C15-C23	–	110.4(6)
Dihedral angle py/im	16.2(3)	14.9(4)

[a] C1m and C5m are the midpoints of the C1–C2 and C5–C6 bonds, respectively.

Moreover, the electronic effects exerted by the R group at N3 are mainly evident in the imidazoline ring, rather than in the metal coordination environment. In fact, in **2c** the N2–C14 and N3–C14 bond lengths of 1.324(7) and 1.336(8) Å are consistent with delocalization in the N2-C14-N3 fragment, while the corresponding values in **3c** (1.283(8), 1.387(9) Å), induced by the tosyl group, indicate quite a short double bond. The degree of delocalization across the amidine is confirmed by the sums of the bond angles about N3 of 359.5° in **2c** versus 349.1° in **3c**.

The chelating ligands are not coplanar, and the distortions are very similar to those found in the Pd complexes with *cis*-disposed phenyl groups.[34] The N1-C13-C14-N2 torsion angles are −13.5(8)° and −16.5(9)° in **2c** and **3c**, respectively, and the phenyl groups on the imidazoline ring avoid an eclipsed conformation through torsion angles C23-C15-C16-C17 of −16.9(7)° (**2c**) and −26.9(9)° (**3c**).

The X-ray structural data show that 1) significant distortions in the imidazoline ring are induced by *cis*-disposed phenyl rings; 2) the N atom in the imidazoline ring bearing a benzyl substituent is planar and shows delocalization in the amidine fragment, as was found with the methyl substituent (see **8a**, Figure 7); and 3) the R substituent influences the coordination of the 1,5-cyclooctadiene *trans* to the pyridine–imidazoline and not the direct coordination of the imidazoline to the rhodium.

Bubbling CO through the reddish solutions of the diolefin complexes displaced the cyclooctadiene ligand and formed yellow solutions of the corresponding bis-carbonyl complexes $[Rh(N–N')(CO)_2]BF_4$ **1d–4d** (Scheme 4).[43] The ^{1}H NMR spectra of the isolated complexes showed the dis-

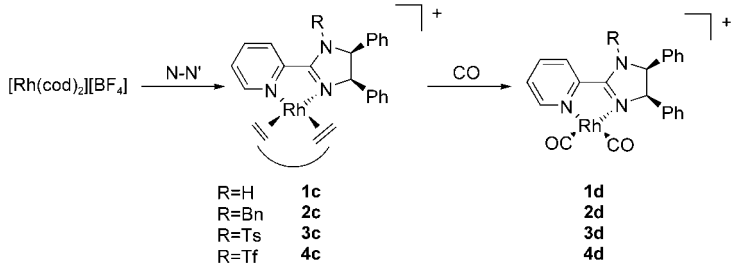

Scheme 4. Synthesis of the Rh^{I} complexes **1c**–**4c**, **1d**–**4d**.

appearance of the signals of 1,5-cyclooctadiene together with a shift of the pyridine–imidazoline signals.

Table 7 lists the CO stretching frequencies of the carbonyl complexes. All the complexes show two bands, assigned to *cis*-bis-carbonyl complexes.[43] The frequencies increase in the order **1**<**2**<**3**<**4**, that is, the basicity of the nitrogen ligands coordinated *trans* to the carbonyls decreases in this order.

Table 7. Selected IR data for $[Rh(CO)_2(N{-}N')]BF_4$ complexes in dichloromethane.

Ligand	ν(CO) [cm^{-1}]	Ligand	ν(CO) [cm^{-1}]
1	2093, 2030	**2**	2093, 2033
3	2104, 2045	**4**	2106, 2050

Copolymerization of carbon monoxide and 4-*tert*-butylstyrene: The copolymerization conditions for isolated complexes **5b**–**10b** were identical to those used for precatalysts **1b**–**4b**,[28] as shown in Table 8. Complexes **6b**–**10b** give rise to efficient catalysts, while **5b** is inactive. The presence of the cyano substituent *ortho* to the coordinating N atom in ligand **5** (Scheme 1), seems to cause enough sterical hindrance to interfere with the chain-growth sequence. A similar behavior was reported for Pd complexes containing 2,9-substituted phenanthrolines and 6-substituted bipyridines.[44]

Table 8. CO/4-*tert*-butylstyrene copolymerization with complexes **1b**–**10b**.[a]

Entry	Cat.	Productivity gCP(gPd)$^{-1}$h^{-1}	M_w (M_w/M_n)	% *l* diads
1[b]	**1b**	2	46400 (1.1)[c]	65
2	**2b**	8.9	74600 (1.5)[c]	52
3	**3b**	7	71100 (1.2)[c]	15
4	**4b**	12.8	59600 (1.5)[c]	18.4
5	**5b**	–	–	–
6	**6b**	3.4	20600 (1.2)[d]	37.3
7	**7b**	4	n.d.[e]	26.4
8	**8b**	5	17600 (1.3)[d]	34.5
9	**9b**	27.2	76600 (1.4)[d]	30.2
10	**10b**	14.6	52400 (2.0)[d]	23

[a] Reaction conditions: n_{cat} = 12.5 μmol; TBS/cat. = 620; room temperature; 1 atm CO; solvent: 5 mL chlorobenzene; t = 24 h. [b] n_{cat} = 8.3 μmol. [b] Determined by SEC-MALLS in THF. [d] Determined by GPC in THF relative to polystyrene standards. [e] n.d. = not determined.

Interestingly, complexes **6b**–**10b** show higher stability in solution during copolymerization than the corresponding **1b**–**5b**. However, the most surprising feature of these catalysts is their disparate productivity, given the similarity of the N ligands. For catalysts **6b**–**10b**, containing the (*R*,*R*)-pyridine–imidazoline ligands, higher productivities are obtained with the less basic systems (**9b** and **10b** are more productive than **6b**–**8b**). However, for catalysts **1b**–**4b**, containing the (*R*,*S*)-ligands, the differences in productivity are less significant. The high productivity observed for complex **9b**, which is an order of magnitude higher than that obtained with other pyridine–imidazoline-derived catalysts (entry 9 vs 1), is noteworthy. The amount of copolymer produced by this system falls in the range of the productivities obtained with the most active systems reported for CO/styrene copolymerization under mild conditions.[15,17]

The size of the polyketones obtained with the new precursors are related to the productivity of the catalyst systems (Table 9). Catalysts **9b** and **10b** yield polyketones with molecular weights up to M_w = 76500 g mol^{-1}, while the more basic catalysts lead to shorter polyketones ($M_w \approx$ 20000 g mol^{-1}). The tacticity of the polyketones was analyzed by integrating the ^{13}C NMR spectra in the $CH(Ph)CH_2$ region (Figure 9). The electronic nature of the substituent in the imidazoline moiety in complexes **1b**–**4b**, influenced the stereoregularity of the polymers (see **1b** vs **4b** in Figure 9). Catalysts **1b** and **2b**, which show *cis* stereochemistry, provided the higher percentage of *l* diads (up to 65%), while catalysts **3b** and **4b** yielded essentially syndiotactic copolymers. With catalysts **6b**–**10b** this effect was less significant, and the content of *l* diads of the polyketones ranged between 23 and 37% (Table 9). Therefore, a prevailing syndiotactic microstructure was obtained with precursors **6b**–**10b**, as previously reported for a similar pyridine–oxazoline ligand.[15,21]

According to the results previously reported,[15,21] the syndiotacticity observed should be produced by chain-end control, which overcomes the enantiosite control created by the chiral ligand. However since a different behavior is observed for the catalysts containing 4′,5′-*cis* and -*trans* imidazolines, we more closely examined the reactivity of the latter towards CO.

Insertion of carbon monoxide into the palladium cationic complexes: Cationic complexes **6b**–**10b** were carbonylated in CD_2Cl_2 solution by bubbling CO for five minutes at 273 K. Selected ^{1}H and ^{13}C NMR data (Table 10) indicate selective formation of acyl carbonyl complexes $[Pd(COMe)(CO)(N{-}N')]BAr'_4$ (**11**–**15**), which result from insertion of CO into the Pd–Me bond (Scheme 5). The ^{1}H NMR spectra at 273 K show two new signals (e.g., for **7b** + CO: δ = 1.72, 1.97 ppm) in the aliphatic region corresponding to Pd–COMe and acetonitrile, respectively. The

Table 9. Selected ^{1}H and ^{13}C NMR resonances for the reaction of complexes **6b–10b** with ^{13}CO.[a]

	T	Me Pd NCMe	Me Pd CO	COMe Pd NCMe	COMe Pd CO
^{1}H NMR					
6b+CO	273	0.51	n.o.	n.o.	1.72
	183				1.53
7b+CO	273	0.49	n.o.	n.o.	1.72
	183				1.55
8b+CO	273	0.44	0.86	1.52 (d)	1.69
	183				1.52
9b+CO	273	M: 0.52 m: 1.04	0.90	1.46 (d)	1.62
	183				1.36
10b+CO	273	M: 0.72 m: 1.15	n.o.	n.o.	2.05 (br)
	183				M: 1.56 m: 2.69 (br)
^{13}C NMR					
6b+CO	183		n.o.	n.o.	173.2, 211.6
7b+CO	273				174.0, 210.5
	183				173.1, 213.3
8b+CO	273		176.3	219.9	174.1, 210.4
	183				173.4, 212.7
9b+CO	273		175.0	215.4	173.2, 206.6
	183				172.5, 208.2
10b+CO	273		n.o.	n.o.	173.2 (br), 207.2 (br)
	183				M:172.3, 208.2 m: 170.3, 212.9

[a] NMR spectra recorded in CD_2Cl_2; n.o.: not observed. M: major isomer, m: minor isomer.

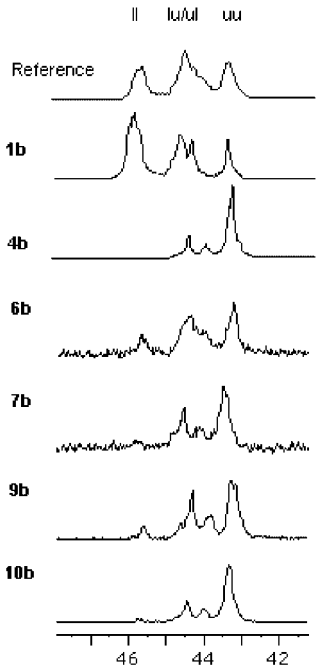

Figure 9. Comparative ^{13}C NMR spectra in the region of the methylene carbon atom of copolymers obtained using the complexes indicated. The reference is an epimerized copolymer.

^{13}C NMR spectra at 273 K show two signals (e.g., for **7b**+CO: $\delta = 174$ and 210.5 ppm) corresponding to Pd–CO and Pd–COMe, respectively.[14]

Variable-temperature NMR experiments were performed in the range 263–183 K for all acyl carbonyl complexes. Complexes **11–14** showed sharp signals over the entire temperature range, that is, they are single isomers. In the case of **15**, the broad signal at 2.05 ppm corresponding to the acyl group disappeared at 233 K. Two doublets became evident at 183 K (at 1.56 and 2.69 ppm; major and minor isomers of **15**, respectively). In the ^{13}C NMR spectrum the initial two signals at 273 K (at 173.2 and 207.2 ppm) became four at 183 K (172.3 and 208.2 for **15** major, 170.3 and 212.9 for **15** minor), as expected for the presence of two acyl carbonyl species. This indicates the presence of *cis*/*trans* equilibrium for acyl carbonyl complex **15** (Scheme 5).

The intermediates of the migratory carbon monoxide insertion were detected in two additional experiments with complexes **8b** and **9b** (Table 10). After CO bubbling at 273 K the tube was carefully placed in the probe without shaking, so that the carbon monoxide could slowly diffuse into the solution. Three more signals in the ^{1}H NMR and two more in the ^{13}C NMR spectrum were observed corresponding to the two intermediate species, which were unequivocally assigned in both cases: the methyl carbonyl (e.g., for **8b**+CO: $\delta(^{1}H) = 0.86$ ppm, $\delta(^{13}C) = 176.3$ ppm) and acyl acetonitrile species (e.g., for **8b**+CO: $\delta(^{1}H) = 1.52$ and 2.35 ppm (due to coordinated acetonitrile), $\delta(^{13}C) = 219.9$ ppm).[14]

The stereochemistry of the acyl carbonyl complexes could not be unequivocally assigned by NOE difference experiments for all the complexes, since in most of the cases interactions were too weak at lower temperatures. Only in the case of complex **12** could *cis* stereochemistry clearly be confirmed, on the basis of NOE interactions between the acyl protons and $H^{4'}$ of the imidazoline moiety. As in the case of the cationic complexes **1b–10b**, whose Pd–Me and Pd–NCMe chemical shifts can be used to establish their stereochemistry, the similarity of the Pd–COMe shifts for complexes **11–14** and **15** (major) suggest that they all have the same stereochemistry.

Conclusion

Modular pyridine–imidazoline ligands **1–10** make it possible to study how the structure of N–N′ ligands influence palladium-catalyzed CO/styrene copolymerization. The basicity of

Table 10. Crystal data and details of structure refinement for compounds **2c**, **3c**, **8a**, and **9a′**.

compound	**2c**	**3c**	**8a**	**9a′**·CH_2Cl_2
formula	$C_{35}H_{35}BF_4N_3Rh$	$C_{35}H_{35}BF_4N_3O_2RhS$	$C_{22}H_{22}ClN_3Pd$	$C_{28}H_{25}Cl_4N_3O_2PdS$
M_r [g mol^{-1}]	687.38	751.44	470.28	715.77
crystal system	monoclinic	monoclinic	orthorhombic	triclinic
space group	$P2_1/n$	$P2_1/c$	$P2_12_12_1$	$P\bar{1}$
a [Å]	11.068(3)	15.071(3)	11.335(3)	9.481(3)
b [Å]	25.636(5)	10.445(5)	13.280(4)	10.207(3)
c [Å]	11.581(4)	20.830(4)	13.327(4)	16.059(4)
α [°]				101.71(2)
β [°]	105.25(2)	99.86(2)		95.82(2)
γ [°]				108.38(2)
V [Å^3]	3170.3(15)	3230.5(18)	2006.1(10)	1421.0(7)
Z	4	4	4	2
ρ_{calcd} [g cm^{-3}]	1.440	1.545	1.557	1.673
$\mu(Mo_{K\alpha})$ [mm^{-1}]	0.591	0.654	1.069	1.135
T [K]	293(2)	293(2)	150(2)	150(2)
$F(000)$	1408	1536	952	720
θ range [°]	2.27–26.02	1.98–25.02	2.36–27.10	2.24–27.10
reflns collected	9764	10603	4678	9780
unique reflns	5285	5604	4252	5805
R(int)	0.0498	0.0709	0.0363	0.0707
observed reflns [$I>2\sigma(I)$]	3202	3483	3681	4239
refined parameters	397	453	246	353
Flack parameter	–	–	−0.04(6)	–
GOF on F^2	1.007	1.038	1.076	1.048
$R1$ [$I>2\sigma(I)$][a]	0.0594	0.0554	0.0539	0.0635
$wR2$ [$I>2\sigma(I)$][a]	0.1579	0.1402	0.1478	0.1914
residuals [e Å^{-3}]	0.942, −0.449	0.614, −0.540	1.137,[b] −1.011	1.407,[b] −1.043

[a] $R_1=\Sigma||F_o|-|F_c||/\Sigma|F_o|$, $wR_2=[\Sigma w(F_o^2-F_c^2)^2/\Sigma w(F_o^2)^2]^{1/2}$. [b] Close to Pd ion.

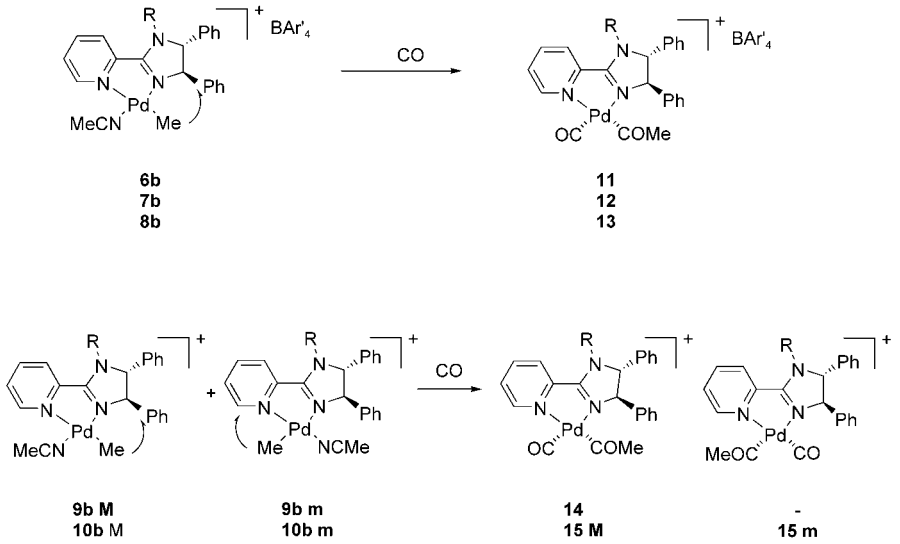

Scheme 5. Carbonylation of the cationic palladium compounds **6b–10b**. M: major isomer; m: minor isomer.

the ligands can be tailored by changing the nature of the remote R substituents on the imidazoline moiety. Modifying the ligand stereochemistry ((*R*,*R*)-4′,5′-*trans* instead of (*R*,*S*)-4′,5′-*cis*) leads to imidazolines with smaller degrees of distortion, as shown by X-ray diffraction. Both structural changes are reflected in the coordination to palladium and rhodium in solution and in the solid state. Density functional calculations on palladium complexes reproduced the experimental observations well.

While all the neutral [PdClMe(N−N′)] complexes are obtained as single *cis* isomers, the stereochemistry of the cationic complexes [PdMe(NCMe)(N−N′)]BAr'_4 depends on the pyridine–imidazoline ligands. Cationic complexes with more basic imidazolines (R = H, Bn, Me) are *cis* isomers, but complexes bearing less basic ligands (R = Ts, Tf) can be present as single *trans* isomers or as mixtures of isomers, depending on the stereochemistry of the imidazoline moiety. This is confirmed by DFT calculations, which show that the electronic effect of the R substituent has an influence on the relative stability of the cationic *cis* and *trans* isomers; this decreases when the electron-withdrawing character of R increases.

Copolymerization data suggest that the structural ligand modifications mentioned above influence the productivity of the catalyst and the stereoregularity of the polymer. Greater stability against reduction during polymerization is observed for the systems containing the less distorted (*R*,*R*)-4′,5′-*trans* imidazolines, although this does not necessarily lead to higher productivity. Here the basicity of the imidazolines also plays an important role: the less basic ligands lead to the most active precursors, probably due to favorable styrene coordination and insertion. The microstructure of the polyketones obtained with the complexes bearing (*R*,*S*)-4′,5′-*cis* imidazolines depends on the electronic nature of the ligand. When (*R*,*R*)-4′,5′-*trans* imidazolines are used, however, syndiotactic polyketones are always obtained, which indicates that chain-end control is more effective than enantiosite control. The size of the polymers does not seem to depend on the structural features of the nitrogen ligands.

Experimental Section

General procedures: All reactions were carried out under nitrogen atmosphere at room temperature by using standard Schlenk techniques. Solvents for synthetic purposes were distilled under nitrogen. Solvents

for spectroscopy were used without further purification. Carbon monoxide (labeled and unlabeled, CP grade, 99%) was supplied by Aldrich. [PdClMe(cod)],[35] $NaBAr'_4$ ($Ar' = 3,5\text{-}(CF_3)_2C_6H_3$),[45] and $[Rh(cod)_2]BF_4$[46] were prepared according to reported methods. ^1H and ^{13}C NMR spectra were recorded on a Varian Gemini spectrometer with a ^1H resonance frequency of 300 MHz and a ^{13}C frequency of 75.4 MHz and on a Varian Mercury VX spectrometer with a ^1H resonance frequency of 400 MHz and a ^{13}C frequency of 100.5 MHz. The resonances were referenced to the solvent peak versus TMS ($CDCl_3$ at $\delta = 7.26$ ppm for ^1H and $\delta = 77.23$ ppm for ^{13}C, CD_2Cl_2 at $\delta = 5.32$ ppm for ^1H and $\delta = 54.0$ ppm for ^{13}C). The NOE experiments were run with a ^1H pulse of 12 μs (300 MHz) or 13.3 μs (400 MHz). Two-dimensional correlation spectra (gCOSY) were obtained with the automatic program of the instrument. Elemental analyses were carried out on a Carlo Erba Microanalyser EA 1108. MS (FAB+) were obtained on a Fisons V6-Quattro instrument. The molecular weights and molecular weight distributions of the copolymers were determined by size-exclusion chromatography on a Waters 515-GPC device using a lineal Waters Ultrastyragel column with a Waters 2410 refractive index detector versus polystyrene standards.

Synthesis of ligands

Compound 5: 2,6-Dicyanopyridine (100 mg, 0.77 mmol) was treated with *meso*-1,2-diphenylethylenediamine (164 mg, 0.77 mmol) in chlorobenzene (5 mL) in the presence of $Yb(OTf)_3$ (46 mg, 0.14 mmol). The mixture was stirred for 24 h under reflux. The desired product was separated from the bis-imidazoline product[30] by column chromatography in 20% yield. $R_f =$ 0.41 (hexane/ethyl acetate 1:2). ^1H NMR (300 MHz, $CDCl_3$, RT): $\delta = 8.58$ (d, $^3J = 7.8$ Hz, 1H; H^5), 7.99 (t, $^3J = 7.8$ Hz, 1H; H^4), 7.83 (d, $^3J = 7.8$ Hz, 1H; H^3), 7.04–6.95 (m, 10H; Ph), 6.49 (s, 1H; NH), 5.58 ppm (br, 2H; $H^{4'}$, $H^{5'}$); ^{13}C NMR (75.4 MHz, $CDCl_3$, RT): $\delta = 162.5$ (s, C^2), 150.0 (s, $C^{2'}$), 138.4 (s, C^6), 130.2 (s, C^3–C^5), 130.0 (s, C^3–C^5), 127.9–127.1 (Ph), 126.2 (s, C^{3-5}), 117.0 (s, C≡N), 67.0 ppm (br, $C^{4'}$, $C^{5'}$); elemental analysis calcd (%) for $C_{21}H_{16}N_4$ (324.4): C 77.76, H 4.97, N 17.27; found: C 77.52, H 4.93, N 17.21.

Compound 6: 2-Cyanopyridine (500 mg, 2.36 mmol) was treated with (1*R*,2*R*)-1,2-diphenylethylenediamine (228 mg, 2.21 mmol) in chlorobenzene (10 mL) in the presence of $Yb(OTf)_3$ (50 mg, 0.16 mmol). The mixture was stirred for 72 h under reflux. The resulting mixture was evaporated to dryness, dissolved in CH_2Cl_2, and washed with three portions of H_2O (15 mL). The organic layers were extracted, dried over $MgSO_4$, and evaporated to give a light-colored solid. Recrystallization from CH_2Cl_2/hexane afforded white crystals in 84% yield. ^1H NMR (300 MHz, $CDCl_3$, RT): $\delta = 8.64$ (d, $^3J = 5.4$ Hz, 1H; H^6), 8.35 (d, $^3J = 8$ Hz, 1H; H^3), 7.85 (t, $^3J = 8$ Hz, 1H; H^4), 7.44 (dd, $^3J = 8$, $^3J = 5.4$ Hz, 1H; H^5), 7.36–7.31 (m, 10H; Ph), 5 (s, 2H; $H^{4'}$, $H^{5'}$); ^{13}C NMR (75.4 MHz, $CDCl_3$, RT): $\delta = 162.7$ (s, C^2), 149 (s, C^6), 148.5 (s, $C^{2'}$), 143.3 (s, Ph), 136.9 (s, C^4), 128.9–126.8 (Ph), 125.6 (s, C^5), 123 (s, C^3), 75.6 (s, $C^{4'}$, $C^{5'}$); elemental analysis calcd (%) for $C_{20}H_{17}N_3$ (299.4): C 80.24, H 5.72, N 14.04; found: C 80.09, H 5.66, N 13.97.

Compound 7: Compound **6** (100 mg, 0.33 mmol) was dissolved in THF (3 mL) and treated with NaH (9.5 mg, 0.4 mmol) for 1 h. Benzyl bromide (42.5 μL, 0.36 mmol) was added dropwise to the reaction mixture at room temperature. After 5 h, evaporation gave a brown paste which was purified by column chromatography to yield a white solid in 71% yield. $R_f = 0.10$ (hexane/ethyl acetate 1:1). ^1H NMR (400 MHz, $CDCl_3$, RT): $\delta =$ 8.72 (ddd, $^3J = 5.5$, $^4J = 1.5$, $^5J = 1.3$ Hz, 1H; H^6), 8.17 (dt, $^3J = 8$, $^4J =$ 1.3 Hz, 1H; H^3), 7.83 (ddd, $^3J = 8$, $^3J = 5.5$, $^4J = 1.5$ Hz, 1H; H^4), 7.4 (m, 1H; H^5), 7.35- 6.97 (m, 15H; Ph), 5.63 (d, $^3J = 15.6$ Hz, 1H; CH_2), 5.0 (d, $^3J = 9.6$ Hz, 1H; $H^{4'}$ or $H^{5'}$), 4.42 (d, $^3J = 9.6$ Hz, 1H; $H^{5'}$ or $H^{4'}$), 3.95 ppm (d, $^3J = 15.6$ Hz, 1H; CH_2); ^{13}C NMR (100.5 MHz, $CDCl_3$, RT): 148.9 (s, C^6), 137.1 (s, C^4), 129.1–127.2 (Ph), 125.4 (s, C^3 or C^5), 124.9 (s, C^5 or C^3), 77.9 (s, $C^{4'}$ or $C^{5'}$), 73.6 (s, $C^{5'}$ or $C^{4'}$), 49.1 ppm (s, CH_2); elemental analysis calcd (%) for $C_{27}H_{23}N_3$ (389.5): C 83.26, H 5.95, N 10.79; found: C 83.02, H 5.92, N 10.74.

Compound 8: This compound was prepared in a similar way to **7** but with MeI as the electrophile, as reported for its enantiomer.[23] ^1H NMR (300 MHz, $CDCl_3$, RT): $\delta = 8.59$ (d, $^3J = 3.6$ Hz, 1H; H^6), 7.99 (d, $^3J =$ 7.9 Hz, 1H; H^3), 7.70 (td, $^3J = 7.9$, $^4J = 1.5$ Hz, 1H; H^4), 7.28–7.15 (m, 11H; H^5, 2Ph), 4.86 (d, $^3J = 10.5$ Hz, 1H; $H^{4'}$ or $H^{5'}$), 4.25 (d, $^3J = 10.5$ Hz, 1H; $H^{4'}$ or $H^{5'}$), 2.88 ppm (s, 3H; CH_3N); elemental analysis calcd (%) for $C_{21}H_{19}N_3$ (313.4): C 80.48, H 6.11, N 13.41; found: C 80.66, H 6.09, N 13.33.

Compound 9: A solution of *p*-toluenesulfonyl chloride (75.7 mg, 0.4 mmol) was added dropwise to a solution of **6** (100 mg, 0.33 mmol) and 4-(dimethylamino)pyridine (73.1 mg, 0.6 mmol) in dichloromethane (3 mL) at 273 K. The reaction mixture was allowed to warm to room temperature and stirred for 5 h. Evaporation of the mixture gave a yellow solid that was purified by column chromatography to obtain a white solid in 77% yield. $R_f = 0.54$ (hexane/ethyl acetate 1/1); ^1H NMR (400 MHz, $CDCl_3$, RT): $\delta = 8.62$ (d, $^3J = 5$ Hz, 1H; H^6), 7.96 (d, $^3J =$ 7.4 Hz, 1H; H^3), 7.84 (t, $^3J = 7.4$ Hz, 1H; H^4), 7.43 (dd, $^3J = 7.4$, $^3J = 5$ Hz, 1H; H^5), 7.39–7.09 (m, 14H; Ph), 5.36 (d, $^3J = 4.8$ Hz, 1H; $H^{4'}$ or $H^{5'}$), 5.17 (d, $^3J = 4.8$ Hz, 1H; $H^{5'}$ or $H^{4'}$), 2.39 ppm (s, 3H; CH_3); ^{13}C NMR (100.5 MHz, $CDCl_3$, RT): $\delta = 158.5$ (s, C^2), 148.6 (s, C^6), 136.5 (s, C^4), 129.1–126.4 (Ph), 125.3 (s, C^5), 124.9 (s, C^3), 78.6 (s, $C^{4'}$ or $C^{5'}$), 72.1 (s, $C^{5'}$ or $C^{4'}$), 21.9 ppm (s, CH_3); elemental analysis calcd (%) for $C_{27}H_{23}N_3O_2S$ (453.6): C 71.50, H 5.11, N 9.26; found: C 70.88, H 5.24, N 9.24.

Compound 10: Similar to the synthesis of **9** but with trifluoromethanesulfonic anhydride as the electrophile. Purification was performed by column chromatography with ethyl acetate as eluent. $R_f = 0.89$; ^1H NMR (400 MHz, $CDCl_3$, RT): $\delta = 8.71$ (dd, $^3J = 4.8$, $^4J = 1.7$ Hz, 1H; H^6), 8.01 (d, $^3J = 7.7$ Hz, 1H; H^3), 7.85 (td, $^3J = 7.7$, $^4J = 1.7$ Hz, 1H; H^4), 7.48–7.31 (m, 11H; H^5, 2Ph), 5.45 (d, $^3J = 3.8$ Hz, 1H; $H^{4'}$ or $H^{5'}$), 5.37 ppm (d, $^3J =$ 3.8 Hz, 1H; $H^{5'}$ or $H^{4'}$); ^{13}C NMR (100.5 MHz, $CDCl_3$, RT): 156.0 (s, C^2), 148.8 (s, C^6), 147.9 (s, $C^{2'}$), 139.9 (s, Ph), 139.4 (s, Ph), 136.7 (s, C^4), 129.3–126.2 (Ph), 125.8 (s, C^5), 124.5 (s, C^3), 78.9 (s, $C^{5'}$ or $C^{4'}$), 72.8 ppm (s, $C^{4'}$ or $C^{5'}$); elemental analysis calcd (%) for $C_{21}H_{16}N_3F_3O_2S$ (431.4): C 58.46, H 3.74, N 9.74; found: C 58.52, H 3.70, N 9.69%.

Synthesis of [PdClMe(N−N′)] (5a–10a): The ligand (**5**–**10**) was added in stoichiometric amount to a solution of [PdClMe(cod)] (50 mg, 0.3 mmol) in toluene (5 mL). The solution was stirred at room temperature for 1 h to give a yellow precipitate in 67% average yield. The precipitate was then collected by filtration and washed with Et_2O.

Compound 5a: ^1H NMR (400 MHz, [D$_6$]acetone, RT): 8.55 (d, $^3J =$ 7.7 Hz, 1H; H^5), 8.46 (s, 1H; NH), 8.32 (t, $^3J = 7.7$ Hz, 1H; H^4), 8.12 (d, $^3J = 7.7$ Hz, 1H; H^3), 7.26–6.85 (m, 10H; Ph), 5.72 (d, $^3J = 11.2$ Hz, 1H; $H^{5'}$), 5.53 (d, $^3J = 11.2$ Hz, 1H; $H^{4'}$), 0.72 ppm (s, 3H; $PdCH_3$).

Compound 6a: ^1H NMR (400 MHz, $CDCl_3$, RT): $\delta = 8.82$ (d, $^3J = 4.7$ Hz, 1H; H^6), 8.60 (s, 1H; NH), 8.41 (d, $^3J = 7.8$ Hz, 1H; H^3), 7.75 (td, $^3J = 7.8$, $^4J = 1.9$ Hz, 1H; H^4), 7.41 (dd, $^3J = 7.8$, $^3J = 4.7$ Hz, 1H; H^5), 7.28–7.16 (m, 10H; Ph), 4.90 (d, $^3J = 6.8$ Hz, 1H; $H^{4'}$), 4.83 ppm (d, $^3J = 6.8$ Hz, 1H; $H^{5'}$), 0.34 (s, 1H; $PdCH_3$); ^{13}C NMR (100.5 MHz, $CDCl_3$, RT): $\delta = 149$ (s, C^6), 138.6 (s, C^4), 129.2–126.2 (Ph), 128.4 (s, C^5), 124.3 (s, C^3), 76.6 (s, $C^{4'}$), 70.3 (s, $C^{5'}$), −8.6 ppm (s, $PdCH_3$); elemental analysis calcd (%) for $C_{21}H_{20}N_3ClPd$ (456.3): C 55.28, H 4.42, N 9.21; found: C 55.59, H 4.47, N 9.30.

Compound 7a: ^1H NMR (400 MHz, $CDCl_3$, RT): $\delta = 9.26$ (d, $^3J = 5$ Hz, 1H; H^6), 7.87 (t, $^3J = 7.8$ Hz, 1H; H^4), 7.76 (d, $^3J = 7.8$ Hz, 1H; H^3), 7.63 (dd, $^3J = 7.8$, $^3J = 5$ Hz, 1H; H^5), 5.15 (d, $^3J = 6.4$ Hz, 1H; $H^{4'}$), 5.02 (d, $^2J = 17.2$ Hz, 1H; CH_2), 4.64 (d, $^3J = 6.4$ Hz, 1H; $H^{5'}$), 4.42 (d, $^2J =$ 17.2 Hz, 1H; CH_2), 0.52 ppm (s, 3H; $PdCH_3$); ^{13}C NMR (100.5 MHz, $CDCl_3$, RT): 150.8 (s, C^6), 138.3 (s, C^4), 129.7–129.1 (Ph), 128.4 (s, C^5), 127.2–126 (Ph), 123.5 (s, C^3), 76.8 (s, $C^{5'}$), 74.3 (s, $C^{4'}$), 50.4 (s, CH_2), −3.4 ppm (s, $PdCH_3$); elemental analysis calcd (%) for $C_{28}H_{26}N_3ClPd$ (546.4): C 61.55, H 4.80, N 7.70; found: C 60.50, H 4.73, N 7.48.

Compound 8a: ^1H NMR (400 MHz, $CDCl_3$, RT): $\delta = 9.28$ (d, $^3J = 4.8$ Hz, 1H; H^6), 8.03 (m, 2H; H^3, H^4), 7.67 (q, $^3J = 4.8$ Hz, 1H; H^5), 7.46- 7.25 (m, 10H; Ph), 5.04 (d, $^3J = 7$ Hz, 1H; $H^{4'}$), 4.58 (d, $^3J = 7$ Hz, 1H; $H^{5'}$), 3.26 (s, 3H; NCH_3), 0.48 (s, 3H; $PdCH_3$); ^{13}C NMR (100.5 MHz, $CDCl_3$, RT): $\delta = 150.8$ (s, C^6), 138.1 (s, C^4), 129.7 (s, Ph), 129.3 (s, C_5), 129.0 (s, Ph), 128.1 (s, Ph), 126.8 (s, Ph), 126.2 (s, Ph), 123.5 (s, C^3), 79.5 (s, $C^{4'}$ or $C^{5'}$), 73.9 (s, $C^{5'}$ or $C^{4'}$), 35.5 (s, CH_3), −7.1 ppm (s, $PdCH_3$); elemental analysis calcd (%) for $C_{22}H_{22}N_3ClPd$ (470.3): C 56.18, H 4.72, N 8.93; found: C 56.30, H 5.01, N 8.87.

Compound 9a: ^1H NMR (400 MHz, $CDCl_3$, RT): $\delta = 9.24$ (d, $^3J = 4$ Hz, 1H; H^6), 8.72 (d, $^3J = 8$ Hz, 1H; H^3), 8.09 (td, $^3J = 8$, $^4J = 1.6$ Hz 1H; H^4), 7.80 (m, 1H; H^5), 7.49–6.91 (m, 14H; Ph), 5.31 (d, $^3J = 5.6$ Hz, 1H; $H^{4'}$), 5.19 (d, $^3J = 5.6$ Hz, 1H; $H^{5'}$), 2.44 (s, 3H; CH_3), 0.55 ppm (s, 3H; $PdCH_3$); ^{13}C NMR (100.5 MHz, $CDCl_3$, RT): $\delta = 150.4$ (s, C^6), 138.3 (s, C^4), 130.6–125.5 (C^3, C^5, Ph), 74.7 (s, $C^{4'}$ or $C^{5'}$), 73.7 (s, $C^{5'}$ or $C^{4'}$), 22.1 (s,

CH_3), −4.9 ppm (s, $PdCH_3$); elemental analysis calcd (%) for $C_{28}H_{26}N_3ClO_2PdS$ (610.5): C 55.09, H 4.29, N 6.88; found: C 55.17, H 4.32, N 6.74.

Compound 10a: ^{1}H NMR (400 MHz, $CDCl_3$, RT): $\delta = 9.29$ (d, $^3J = 4.7$ Hz, 1H; H^6), 8.22 (d, $^3J = 7.7$ Hz, 1H; H^3), 8.10 (td, $^3J = 7.7$ Hz, $^4J = 1.7$ Hz, 1H; H^4), 7.84 (dd, $^3J = 7.7$ Hz, $^3J = 4.7$ Hz, 1H; H^5), 7.47–7.35 (m, 10H; Ph), 5.55 (d, $^3J = 1.8$ Hz, 1H; $H^{4'}$), 5.43 (d, $^3J = 1.8$ Hz, 1H; $H^{5'}$), 0.75 ppm (s, 3H; $PdCH_3$); ^{13}C NMR (100.5 MHz, $CDCl_3$, RT): $\delta = 150.5$ (s, C^6), 138.4 (s, C^4), 130.1 (s, C^5), 130.0 (s, Ph), 129.6 (s, Ph), 129.5 (s, C^3), 125.8 (s, Ph), 125.4 (s, Ph), 75.8 (s, $C^{4'}$ or $C^{5'}$), 75.5 (s, $C^{5'}$ or $C^{4'}$), −3.7 ppm (s, $PdCH_3$); elemental analysis calcd (%) for $C_{22}H_{19}N_3ClF_3O_2PdS$ (588.3): C 44.91, H 3.26, N 7.14; found: C 44.80, H 3.42, N 7.20.

Synthesis of [PdMe(NCMe)(N−N′)]BAr′$_4$ (5b–10b): A stoichiometric amount of $NaBAr'_4$ was added together with MeCN (0.5 mL) to a solution of [PdClMe(N−N′)] (0.3 mmol) in CH_2Cl_2 (5 mL). The light yellow solution that formed was stirred for 1 h, filtered through kieselghur, and evaporated to dryness. The light yellow compounds were crystallized from CH_2Cl_2/hexane in 76% average yield.

Compound 5b: ^{1}H NMR (400 MHz, $CDCl_3$, RT): $\delta = 9.05$ (s, 1H; NH), 7.91 (m, 2H; H^4, H^5), 7.79 (s, $^3J = 7.6$ Hz, 1H; H^3), 7.69 (s, 8H; H^b), 7.51 (s, 4H; H^d), 7.13–6.79 (m, 10H; Ph), 5.70 (d, $^3J = 11.2$ Hz, 1H; $H^{5'}$), 5.50 (d, $^3J = 11.2$ Hz, 1H; $H^{4'}$), 2.33 (s, 3H; $PdNCCH_3$), 0.90 ppm (s, 3H; $PdCH_3$).

Compound 6b: ^{1}H NMR (400 MHz, $CDCl_3$, RT): $\delta = 8.34$ (d, $^3J = 4.8$ Hz, 1H; H^6), 7.84 (t, $^3J = 8$ Hz, 1H; H^4), 7.70 (s, 8H; H^b), 7.64 (d, $^3J = 8$ Hz, 1H; H^3), 7.45 (s, 4H; H^d), 7.43–7.20 (m, 11H; H^5, 2Ph), 6.31 (s, 1H; NH), 5.05 (d, $^3J = 7$ Hz, 1H; $H^{4'}$), 4.96 (d, $^3J = 7$ Hz, 1H; $H^{5'}$), 2.30 (s, 3H; $PdNCCH_3$), 0.56 ppm (s, 3H; $PdCH_3$); ^{13}C NMR (100.5 MHz, $CDCl_3$, RT): $\delta = 161.6$ (q, ^1J (C-B) = 197.2 Hz, C^a), 149.2 (s, C^6), 139.9 (s, C^4), 134.8 (s, C^b), 129.8 (s, Ph), 129.7 (s, Ph), 129.5 (s, Ph), 129.4 (s, Ph), 129.2 (m, C^e), 128.9 (s, C_5), 126.1 (s, Ph), 123.3 (s, C^3), 117.6 (s, C^d), 76.6 (s, $C^{4'}$), 70.7 (s, $C^{5'}$), 3.4 (s, $PdNCCH_3$), −3.1 ppm (s, $PdCH_3$); MS (FAB): *m/z*: 703.2 $[M-Me-NCMe+\mathbf{6}]^{2+}$, 404.1 $[M-Me-NCMe]^+$, 298.1 $[\mathbf{6}]^+$; elemental analysis calcd (%) for $C_{55}H_{35}N_4BF_{24}Pd$ (1325.1): C 49.85, H 2.66, N 4.23; found: C 50.02, H 2.60, N 4.14.

Compound 7b: ^{1}H NMR (400 MHz, $CDCl_3$, RT): $\delta = 8.38$ (d, $^3J = 4$ Hz, 1H; H^6), 7.84 (m, 2H; H^4, H^5), 7.70 (s, 8H; H^b), 7.51 (s, 4H; H^d), 7.45–7.02 (m, 16H; H^3, 15Ph), 5.05 (d, $^3J = 5.6$ Hz, 1H; $H^{4'}$), 5.02 (d, $^3J = 17.2$ Hz, 1H; CH_2), 4.72 (d, $^3J = 5.6$ Hz, 1H; $H^{5'}$), 4.46 (d, $^3J = 17.2$ Hz, 1H; CH_2), 2.28 (s, 3H; $PdNCCH_3$), 0.54 ppm (s, 3H; $PdCH_3$); ^{13}C NMR (100.5 MHz, $CDCl_3$, RT): $\delta = 161.7$ (q, $^1J_{C\text{-}B} = 197.2$ Hz, C^a), 149.6 (s, C^6), 139.9 (s, C^4), 134.8 (s, C^b), 130.0 (s, Ph), 129.6 (s, Ph), 129.5 (s, Ph), 129.0 (s, C^5), 128.8 (m, C^e), 127.0 (s, Ph), 126.1 (s, Ph), 125.6 (Ph), 124.9 (s, C^3), 117.6 (s, C^d), 76.8 (s, $C^{4'}$ or $C^{5'}$), 73.6 (s, $C^{5'}$ or $C^{4'}$), 50.1 (s, CH_2), 3.4 (s, $PdNCCH_3$), −2.2 ppm (s, $PdCH_3$); MS (FAB): *m/z*: 883.3 $[M-Me-NCMe+\mathbf{7}]^{2+}$, 494.1 $[M-Me-NCMe]^+$, 390.2 $[\mathbf{7}]^+$; elemental analysis calcd (%) for $C_{62}H_{41}N_4BF_{24}Pd$ (1415.2): C 52.62, H 2.92, N 3.96; found: C 52.35, H 3.00, N 3.83.

Compound 8b: ^{1}H NMR (400 MHz, $CDCl_3$, RT): $\delta = 8.38$ (d, $^3J = 4$ Hz, 1H; H^6), 8.03 (d, $^3J = 8$ Hz, 1H; H^3), 7.86 (t, $^3J = 8$ Hz, 1H; H^4), 7.69 (s, 8H; H^b), 7.5 (s, 4H; H^d), 7.46- 7.19 (m, 11H; H^5, 2Ph), 4.92 (d, $^3J = 7.2$ Hz, 1H; $H^{5'}$), 4.64 (d, $^3J = 7.2$ Hz, 1H; $H^{4'}$), 3.25 (s, 3H; NCH_3), 2.30 (s, 3H; $PdNCCH_3$), 0.48 ppm (s, 3H; $PdCH_3$); ^{13}C NMR (100.5 MHz, $CDCl_3$, RT): $\delta = 161.6$ (q, $^1J_{C\text{-}B} = 197.2$ Hz, C^a), 149.6 (s, C^6), 139.7 (s, C^4), 134.8 (s, C^b), 130.0 (s, Ph), 129.8 (s, Ph), 129.4 (s, Ph), 129.2 (m, C^e), 128.9 (s, Ph), 128.7 (s, C^5), 126.6 (s, Ph), 125.9 (s, Ph), 124.7 (s, C^3), 117.6 (s, C^d), 79.3 (s, $C^{4'}$), 73.5 (s, $C^{5'}$), 35.1 (s, CH_3N), 3.5 (s, 1C, $PdNCCH_3$), −2.5 ppm (s, 1C, $PdCH_3$); MS (FAB): *m/z*: 731.2 $[M-Me-NCMe+\mathbf{8}]^{2+}$, 418.1 $[M-Me-NCMe]^+$, 314.2 $[\mathbf{8}]^+$; elemental analysis calcd (%) for $C_{56}H_{37}N_4BF_{24}Pd$ (1339.3): C 50.23, H 2.78, N 4.18; found: C 49.35, H 3.03, N 3.99.

Compound 9b: ^{1}H NMR (400 MHz, $CDCl_3$, RT): Ratio major/minor = 3:1; major: $\delta = 8.62$ (d, $^3J = 8$ Hz, 1H; H^3), 8.35 (dd, $^3J = 5$, $^4J = 1.3$ Hz, 1H; H^6), 8.05 (td, $^3J = 8$, $^4J = 1.3$ Hz, 1H; H^4), 7.71 (s, 8H; H^b), 7.52 (s, 5H; H^5, 4H^d), 7.50–6.80 (m, 14H; Ph), 5.36 (d, $^3J = 3.2$ Hz, 1H; $H^{5'}$), 5.06 (d, $^3J = 3.2$ Hz, 1H; $H^{4'}$), 2.41 (s, 3H; CH_3Ts), 2.20 (s, 3H; $PdNCCH_3$), 0.57 ppm (s, 3H; $PdCH_3$); ^{13}C NMR (100.5 MHz, $CDCl_3$, RT): $\delta = 161.7$ (q, $^1J_{C\text{-}B} = 198.1$ Hz, C^a), 149.3 (s, C^6), 140.1 (s, C^4), 134.8 (s, C^b), 130.8–123.2 (C^3, C^4, Ph), 117.6 (s, C^d), 74.3 (s, $C^{5'}$), 74.1 (s, $C^{4'}$), 22.0 (s, CH_3), 3.2 (s, $PdNCCH_3$), −0.03 ppm (s, $PdCH_3$); minor: $\delta = 8.63$ (d, $^3J = 8.2$ Hz, 1H; H^3), 8.50 (d, $^3J = 4.4$ Hz, 1H; H^3), 8.17 (td, $^3J = 8.2$, $^4J = 1.6$ Hz, 1H; H^4), 7.71 (s, 9H; H^5, 8H^b), 7.52 (s, 4H; H^d), 7.50–6.80 (m, 14H; Ph), 5.24 (d, $^3J = 4.8$ Hz, 1H; $H^{5'}$), 5.08 (d, $^3J = 4.8$ Hz, 1H; $H^{4'}$), 2.45 (s, 3H; CH_3Ts), 1.61 (s, 3H; $PdNCCH_3$), 0.97 ppm (s, 3H; $PdCH_3$); ^{13}C NMR (100.5 MHz, $CDCl_3$, RT): $\delta = 161.7$ (q, $^1J_{C\text{-}B} = 198.1$ Hz, C^a), 147.2 (s, C^6), 137.8 (s, C^4), 134.8 (s, 8C, C^b), 130.8- 123.2 (C^3, C^4, Ph), 117.6 (s, 4C, C^d), 76.4 (s, C^4), 74.1 (s, $C^{5'}$), 22.0 (s, CH_3), 5.67 (s, $PdCH_3$), 2.44 ppm (s, $PdNCCH_3$); elemental analysis calcd (%) for $C_{62}H_{41}N_4BClF_{24}O_2PdS$ (1514.9): C 50.34, H 2.79, N 3.79; found: C 50.21, H 2.68, N 3.66.

Compound 10b: ^{1}H NMR (400 MHz, $CDCl_3$, RT): Ratio major/minor = 2:1; major: $\delta = 8.38$ (d, $^3J = 5.2$ Hz, 1H; H^6), 8.28 (d, $^3J = 7.9$ Hz, 1H; H^3), 8.04 (td, $^3J = 7.9$, $^4J = 1.6$ Hz, 1H; H^4), 7.70 (s, 8H; H^b), 7.51 (s, 4H; H_d), 7.48–7.14 (m, 11H; H^5, 2Ph), 5.55 (d, $^3J = 2.2$ Hz, 1H; $H^{5'}$), 5.28 (d, $^3J = 2.2$ Hz, 1H; $H^{4'}$), 2.26 (s, 3H; $PdNCCH_3$), 0.74 ppm (s, 3H; $PdCH_3$); ^{13}C NMR (100.5 MHz, $CDCl_3$, RT): $\delta = 161.7$ (q, $^1J_{C\text{-}B} = 198.1$ Hz, C^a), 149.6 (s, C^6), 140.1 (s, C^4), 134.8 (s, C^b), 130.7–123.2 (C^5, C^3, C^e, Ph), 117.6 (s, C^d), 77.4 (s, $C^{4'}$ or $C^{5'}$), 75.5 (s, $C^{5'}$ or $C^{4'}$), 3.3 (s, $PdCH_3$), 0.9 ppm (s, $PdNCCH_3$); minor: $\delta = 8.52$ (d, $^3J = 5.8$ Hz, 1H; H^6), 8.29 (m, 1H; H^3), 8.18 (td, $^3J = 7.9$, $^4J = 1.3$ Hz, 1H; H^4), 7.74 (dd, $^3J = 7.9$, $^3J = 5.8$ Hz, 1H; H^5), 7.70 (s, 8H; H^b), 7.51 (s, 4H; H^d), 7.48–7.14 (m, 10H; Ph), 5.53 (d, $^3J = 3.4$ Hz, 1H; $H^{5'}$), 5.32 (d, $^3J = 3.4$ Hz, 1H; $H^{4'}$), 1.73 (s, 3H; $PdNCCH_3$), 1.07 ppm (s, 3H; $PdCH_3$); ^{13}C NMR (100.5 MHz, $CDCl_3$, RT): 161.7 (q, $^1J_{C\text{-}B} = 198.1$ Hz, C^a), 150.4 (s, C^6), 140.4 (s, C^4), 134.8 (s, C^b), 130.7–123.2 (C^5, C^3, C^e, Ph), 117.6 (s, C^d), 75.7 (s, $C^{4'}$ or $C^{5'}$), 75.2 (s, $C^{4'}$ or $C^{5'}$), 6.8 (s, $PdCH_3$), 2.6 ppm (s, $PdNCCH_3$); elemental analysis calcd (%) for $C_{56}H_{34}N_4BF_{27}O_2PdS$ (1457.3): C 46.16, H 2.35, N 3.84; found: C 46.36, H 2.60, N 3.10.

Synthesis of [Rh(cod)(N−N′)]BF$_4$: When the pyridine–imidazoline ligands **1**–**4** (0.12 mmol) were added to a reddish solution of $[Rh(cod)_2]BF_4$ (0.12 mmol) in CH_2Cl_2 (2 mL), the color changed instantaneously. After 5 min, diethyl ether (5 mL) was added to precipitate complexes **1c**–**4c**. Average yield: 74%.

Compound 1c: ^{1}H NMR (400 MHz, $CDCl_3$, RT): $\delta = 8.57$ (d, $^3J = 7.8$ Hz, 1H; H^3), 8.39 (s, 1H; NH), 8.22 (dd, $^3J = 7.8$, $^3J = 6.9$ Hz, 1H; H^4), 7.78 (d, $^3J = 5.6$ Hz, 1H; H^6), 7.67 (dd, $^3J = 6.9$, $^3J = 5.6$ Hz, H^5), 7.08–6.83 (m, 10H; Ph), 5.74 (d, $^3J = 11.7$ Hz, 1H; $H^{4'}$ or $H^{5'}$), 5.25 (d, $^3J = 11.7$ Hz, 1H; $H^{5'}$ or $H^{4'}$), 4.44 (m, 1H; CH= cod), 4.17 (m, 2H; CH= cod), 3.51 (m, 1H; CH= cod), 2.51–2.37 (m, 4H; CH_2 cod), 1.90–1.68 ppm (m, 4H; CH_2 cod); elemental analysis calcd (%) for $C_{28}H_{29}N_3BF_4Rh$ (597.4): C 56.29, H 4.89, N 7.03; found: C 56.14, H 4.96, N 6.70.

Compound 2c: ^{1}H NMR (400 MHz, $CDCl_3$, RT): $\delta = 8.37$ (d, $^3J = 8$ Hz, 1H; H^3), 8.27(t, $^3J = 8$ Hz, 1H; H^4), 7.91 (d, $^3J = 5.5$ Hz, 1H; H^6), 7.79 (dd, $^3J = 8$, $^3J = 5.5$ Hz, 1H; H^5), 5.47 (d, $^3J = 12$ Hz, 1H; $H^{4'}$ or $H^{5'}$), 5.32 (d, $^3J = 17.2$ Hz, 1H; CH_2), 5.2 (d, $^3J = 12$ Hz, 1H; $H^{5'}$ or $H^{4'}$), 4.55 (d, $^3J = 17.2$ Hz, 1H; CH_2), 4.41 (m, 1H; CH= cod), 4.31 (m, 1H; CH= cod), 4.22 (m, 1H; CH= cod), 3.56 (m, 1H; CH= cod), 2.5 (m, 2H; CH_2 cod), 2.3 (m, 2H; CH_2 cod), 1.97 (m, 2H; CH_2 cod), 1.8 ppm (m, 2H; CH_2 cod); elemental analysis calcd (%) for $C_{35}H_{35}N_3BF_4Rh$ (687.6): C 61.14, H 5.13, N 6.11; found: C 61.03, H 5.24, N 5.56.

Compound 3c: ^{1}H NMR (300 MHz, $CDCl_3$, RT): $\delta = 8.56$ (d, $^3J = 8.1$ Hz, 1H; H^3), 8.34 (m, 1H; H^4), 8.04 (m, 2H; H^5, H^6), 7.76 (d, $^2J = 8.3$ Hz, 2H; ArH Ts), 7.45 (d, $^2J = 8.3$ Hz, 2H; ArH Ts), 7.06–6.67 (m, 10H; Ph), 5.96 (d, $^3J = 9.5$ Hz, 1H; $H^{4'}$ or $H^{5'}$), 5.37 (d, $^3J = 9.5$ Hz, 1H; $H^{5'}$ or $H^{4'}$), 4.34 (m, 4H; CH= cod), 2.3 (m, 4H; CH_2 cod), 1.81 ppm (m, 4H; CH_2 cod); elemental analysis calcd (%) for $C_{35}H_{35}N_3BF_4SO_2Rh$ (751.6): C 55.9, H 3.19, N 5.59; found: C 55.75, H 3.78, N 5.58.

Compound 4c: ^{1}H NMR (400 MHz, $CDCl_3$, RT): $\delta = 8.30$ (m, 2H; H^6, H^3), 8.14 (m, 1H; H^4 or H^5), 8.10 (m, 1H; H^5 or H^4), 7.15 (m, 6H; Ph), 7.00 (br, 1H; Ph), 6.72 (m, 2H; Ph), 6.52 (br, 1H; Ph), 6.12 (d, $^3J = 8.8$ Hz, 1H; $H^{4'}$ or $H^{5'}$), 5.95 (d, $^3J = 8.8$ Hz, 1H; $H^{5'}$ or $H^{4'}$), 4.56 (m, 2H; CH= cod), 3.96 (m, 2H; CH= cod), 2.43 (m, 2H; CH_2 cod), 2.31 (m, 2H; CH_2 cod), 1.85 ppm (m, 4H; CH_2 cod).

Synthesis of [Rh(CO)$_2$(N−N′)]BF$_4$ (1d–4d): Bubbling carbon monoxide through solutions of **1c**–**4c** (0.3 mmol) in CH_2Cl_2 (5 mL) led to the formation of yellow solutions of the dicarbonyl complexes, which were precipitated by adding Et_2O (5 mL).

Compound 1d: ^{1}H NMR (300 MHz, $CDCl_3$, RT): $\delta = 9.08$ (s, 1H; NH), 8.84 (d, $^3J = 8.4$ Hz, 1H; H^3), 8.65 (d, $^3J = 5.3$ Hz, 1H; H^6), 8.43 (dd, $^3J = 8.4$ Hz, $^3J = 7.1$ Hz, 1H; H^4), 7.82 (dd, $^3J = 7.1$ Hz, $^3J = 5.3$ Hz, 1H; H^5),

7.13- 6.92 (m, 10H; Ph), 5.83 (d, $^3J=12.2$ Hz, 1H; $H^{4'}$ or $H^{5'}$), 5.67 ppm (d, $^3J=12.2$ Hz, 1H; $H^{5'}$ or $H^{4'}$).

Compound 2d: ^{1}H NMR (400 MHz, $CDCl_3$, RT): $\delta=8.72$ (d, $^3J=4.8$ Hz, 1H; H^6), 8.44 (d, $^3J=8$ Hz, 1H; H^3), 8.38 (t, $^3J=8$ Hz, 1H; H_4), 7.82 (dd, $^3J=8$ Hz, $^3J=4.8$ Hz, 1H; H^5), 7.37–6.89 (m, 15H; Ph), 5.72 (d, $^3J=$ 12.4 Hz, 1H; $H^{4'}$ or $H^{5'}$), 5.58 (m, 2H; $H^{5'}$ or $H^{4'}$, CH_2), 4.64 ppm (d, $^3J=$ 17.2 Hz, 1H; CH_2).

Compound 3d: ^{1}H NMR (400 MHz, $CDCl_3$, RT): $\delta=8.86$ (m, 2H; H^6, H^3), 8.49 (t, $^3J=8$ Hz, 1H; H^4), 8.04 (t, $^3J=6.6$ Hz, 1H; H^5), 7.78 (d, $^2J=$ 8.2 Hz, 2H; ArH Ts), 7.41 (d, $^2J=8.2$ Hz, 2H; ArH Ts), 7.16–6.74 (m, 10H; Ph), 5.98 (d, $^3J=9.6$ Hz, 1H; $H^{4'}$ or $H^{5'}$), 5.71 ppm (d, $^3J=9.6$ Hz, 1H; $H^{5'}$ or $H^{4'}$).

Compound 4d: ^{1}H NMR (400 MHz, $CDCl_3$, RT): $\delta=8.92$ (d, $^3J=5.3$ Hz, 1H; H^6), 8.50 (d, $^3J=7.8$ Hz, 1H; H^3), 8.42 (td, $^3J=7.8$, $^4J=1.2$ Hz, 1H; H^4), 8.09 (ddd, $^3J=7.8$, $^3J=5.3$ Hz, $^4J=1.2$ Hz, 1H; H^5), 7.18 (m, 8H; Ph), 6.84 (m, 2H; Ph), 5.58 ppm (m, 2H; $H^{4'}$ and $H^{5'}$).

X-ray crystallography: Crystal data and data-collection and refinement parameters are summarized in Table 10. All data sets were colllected out on a Nonius DIP-1030H system with graphite-monochromatized $Mo_{K\alpha}$ radiation ($\lambda=0.71073$ Å). For each compound a total of 30 frames were collected with an exposure time of 12–20 min, rotation of 6° about φ, with the detector 90 mm from the crystal. Cell refinement, indexing, and scaling of the data sets were carried out with the programs Mosflm and Scala.[47]

All structures were solved by Patterson and Fourier analyses[48] and refined by the full-matrix least-squares method based on F^2 for all observed reflections. The final cycles include the contribution of hydrogen atoms at calculated positions. In **3c** the BF_4^- anion was found to be disordered over two positions corresponding to rotation about a B–F bond with refined occupancies of 0.59(2)/0.41(2). A molecule of CH_2Cl_2 was detected in the ΔF map of **9a′**. All calculations were performed with the WinGX System, Ver 1.64.02.[49]

CCDC 234657–234660 contain the supplementary crystallographic data for this paper. These data can be obtained free of charge via www.ccdc.cam.ac.uk/conts/retrieving.html (or from the Cambridge Crystallographic Data Centre, 12 Union Road, Cambridge CB2 1EZ, UK; fax: (+44) 1223-336-033; or deposit@ccdc.cam.uk).

Computational details: DFT calculations were carried with the Amsterdam density functional program (ADFv2000), developed by Baerends et al.[50,51] The numerical integration scheme used in the calculations was developed by te Velde et al.,[52,53] and the geometry-optimization algorithms were those implemented by Versluis and Ziegler.[54] A triple-zeta plus polarization Slater-type basis set, as included in the ADF library, described the electronic configurations of the molecular systems. The 1s–3d electrons for Pd, the 1s electrons for C, O, N, and the 2p electrons for Cl were treated as frozen cores. Geometry was fully optimized using nonlocal corrections self-consistently. The DFT functional was the local VWN exchange-correlation potential with Becke's nonlocal exchange-correlation corrections[55] and Perdew's correlation corrections[56] (BP86). Relativistic effects were considered by using the scalar zeroth-order regular approximation (ZORA).[57] No symmetry constraints were used. We treated most atoms at this QM level, but used QM/MM calculations to include only the phenyl substituents of the imidazoline group, which are described in the MM partition. QM/MM calculations were performed by applying the IMOMM method[58] as implemented in the ADF package.[59] SYBIL[60] force field was used as implemented in ADF to describe the atoms included in the MM part. For the palladium atom, we used UFF parameters from the literature.[61] The ratio between the P–C(aromatic) and the P–H bond length was set to 1.234 Å.

Acknowledgement

The Ministerio de Ciencia y Tecnología (BQU 2001-0656) is acknowledged for financial support and for a grant (to A.B.). The "Palladium" Network, HPRN-CT-2002-00196 and the COST D-17 Action are also acknowledged.

[1] For recent reviews on late-transition metal catalyzed polymerizations, see a) S. D. Ittel, L. K. Johnson, M. Brookhart, *Chem. Rev.* **2000**, *100*, 1169–1203; b) S. Mecking, *Coord. Chem. Rev.* **2000**, *203*, 325–351.
[2] E. Drent, P. H. M. Budzelaar, *Chem. Rev.* **1996**, *96*, 663–681.
[3] K. Nozaki, T. Hiyama, *J. Organomet. Chem.* **1999**, *576*, 248–253.
[4] C. Bianchini, A. Meli, *Coord. Chem. Rev.* **2002**, *225*, 35.
[5] a) F. C. Rix, M. Brookhart, P. S. White, *J. Am. Chem. Soc.* **1996**, *118*, 4746–4764; b) C. S. Shultz, J. Ledford, J. M. DeSimone, M. Brookhart, *J. Am. Chem. Soc.* **2000**, *122*, 6351–6356; c) J. Ledford, C. S. Shultz, D. P. Gates, P. S. White, J. M. DeSimone, M. Brookhart, *Organometallics* **2001**, *20*, 5266–5276.
[6] K. Nozaki, H. Komaki, Y. Kawashima, T. Hiyama, T. Matsubara, *J. Am. Chem. Soc.* **2001**, *123*, 534–544.
[7] K. R. Reddy, K. Surekha, G. H. Lee, S. M. Peng, J. T. Chen, S. T. Liu, *Organometallics* **2001**, *20*, 1292–1299.
[8] a) C. Carfagna, G. Gatti, D. Martini, C. Pettinari, *Organometallics* **2001**, *20*, 2175–2182; b) B. Binotti, C. Carfagna, G. Gatti, D. Martini, L. Mosca, C. Pettinari, *Organometallics* **2003**, *22*, 1115–1123.
[9] M. A. Zuideveld, P. C. J. Kamer, P. W. N. M. van Leeuwen, P. A. A. Klusener, H. A. Stil, C. F. Roobeek, *J. Am. Chem. Soc.* **1998**, *120*, 7977–7978.
[10] G. K. Barlow, J. D. Boyle, N. A. Cooley, T. Ghaffar, D. F. Wass, *Organometallics* **2000**, *19*, 1470–1476.
[11] G. Consiglio, B. Milani in *Catalytic Synthesis of Alkene–Carbon Monoxide Copolymers and Cooligomers* (Ed.: A. Sen), Kluwer Academic, Dordrecht, **2003**, pp. 189–215.
[12] P. Corradini, C. De Rosa, A. Panunzi, G. Petrucci, P. Pino, *Chimia* **1990**, *44*, 52–54.
[13] M. Barsacchi, G. Consiglio, L. Medici, G. Petrucci, U. W. Suter, *Angew. Chem.* **1991**, *103*, 992; *Angew. Chem. Int. Ed. Engl.* **1991**, *30*, 989; an exception to this behavior can be found in J.-C. Yuan, S.-J. Lu, *Organometallics* **2001**, *20*, 2697–2703.
[14] M. Brookhart, F. C. Rix, J. M. DeSimone, J. C. Barborak, *J. Am. Chem. Soc.* **1992**, *114*, 5894–5895.
[15] M. Brookhart, M. I. Wagner, G. G. A. Balavoine, H. A. Haddou, *J. Am. Chem. Soc.* **1994**, *116*, 3641–3642.
[16] S. Bartolini, C. Carfagna, A. Musco, *Macromol. Rapid Commun.* **1995**, *16*, 9–14.
[17] M. T. Reetz, G. Haderlein, K. Angermund, *J. Am. Chem. Soc.* **2000**, *122*, 996–997.
[18] B. Milani, G. Corso, G. Mestroni, C. Carfagna, M. Formica, R. Seraglia, *Organometallics* **2000**, *19*, 3435–3441.
[19] B. Milani, A. Scarel, G. Mestroni, S. Gladiali, R. Taras, C. Carfagna, L. Mosca, *Organometallics* **2002**, *21*, 1323–1325.
[20] A. Bastero, A. Ruiz, J. A. Reina, C. Claver, A. M. Guerrero, F. A. Jalón, B. R. Manzano, *J. Organomet. Chem.* **2001**, *619*, 287–292.
[21] A. Aeby, G. Consiglio, *Inorg. Chim. Acta* **1999**, *296*, 45–51, and references therein.
[22] G. Helmchen, A. Pfaltz, *Acc. Chem. Res.* **2000**, *33*, 336, and references therein.
[23] A. J. Davenport, D. L. Davies, J. Fawcett, D. R. Russell, *J. Chem. Soc. Perkin Trans.* 1 **2001**, *1*, 1500–1503.
[24] a) B. Çetinkaya, E. Çetinkaya, P. B. Hitchcock, M. F. Lappert, I. Özdemir, *J. Chem. Soc. Dalton Trans.* **1997**, 1359–1362; b) B. Çetinkaya, B. Alici, I. Özdemir, C. Bruneau, P. H. Dixneuf, *J. Organomet. Chem.* **1999**, *575*, 187.
[25] C. Botteghi, A. Schionato, G. Chelucci, H. Brunner, A. Kürzinger, U. Obermann, *J. Organomet. Chem.* **1989**, *370*, 17.
[26] N. A. Boland, M. Casey, S. J. Hynes, J. W. Matthews, M. P. Smyth, *J. Org. Chem.* **2002**, *67*, 3919–3922, and references therein.
[27] J. Elguero, E. Gonzalez, J. L. Imbach, R. Jacquier, *Bull. Soc. Chim. Fr.* **1969**, *11*, 4075–4077.
[28] A. Bastero, S. Castillón, C. Claver, A. Ruiz, *Eur. J. Inorg. Chem.* **2001**, *12*, 3009–3011.
[29] a) A. Batistini, G. Consiglio, U. W. Suter, *Angew. Chem.* **1992**, *104*, 306; *Angew. Chem. Int. Ed. Engl.* **1992**, *31*, 303; b) B. Sesto, G. Consiglio, *Chem. Commun.* **2000**, 1011–1012.
[30] G. Chelucci, S. Deriu, G. A. Pinna, A. Saba, R. Valenti, *Tetrahedron: Asymmetry* **1999**, *10*, 3803.

[31] C. Bianchini, H. M. Lee, A. Meli, W. Oberhauser, M. Peruzzini, F. Vizza, *Organometallics* **2002**, *21*, 16–33.
[32] B. Sesto, G. Consiglio, *J. Am. Chem. Soc.* **2001**, *123*, 4097–4098.
[33] H. Günther, *NMR Spectroscopy. Basic Principles, Concepts and Applications in Chemistry*, Wiley, Chichester, **1995**.
[34] A. Bastero, A. Ruiz, C. Claver, B. Milani, E. Zangrando, *Organometallics* **2002**, *21*, 5820–5829.
[35] R. E. Rülke, J. M. Ernsting, A. L. Spek, C. J. Elsevier, P. W. N. M. van Leeuwen, K. Vrieze, *Inorg. Chem.* **1993**, *32*, 5769–5778.
[36] P. Pelagatti, M. Carcelli, F. Franchi, C. Pelizzi, A. Bacchi, H.-W. Frühauf, K. Goubitz, K. Vrieze, *Eur. J. Inorg. Chem.* **2000**, 463–475.
[37] A similar reaction was observed in the crystallization of complex **2a**. See ref. [34].
[38] V. De Felice, V. G. Albano, C. Castellari, M. E. Cucciolito, A. De Renzi, *J. Organomet. Chem.* **1991**, *403*, 269.
[39] See Supporting Information.
[40] Low-temperature NMR studies confirmed the presence of a single isomer for complexes **1b**–**8b**.
[41] J. Elguero, A. Guerrero, F. Gómez de la Torre, A. de la Hoz, F. A. Jalón, B. R. Manzano, A. Rodríguez, *New J. Chem.* **2001**, *25*, 1050–1060.
[42] a) S. W. Kaiser, R. B. Saillant, W. M. Butler, P. G. Rasmussen, *Inorg. Chem.* **1976**, *15*, 2681–2688; b) H. Brunner, R. Storiko, F. Rominger, *Eur. J. Inorg. Chem.* **1998**, *6*, 771–781; c) B. de Bruin, R. J. N. A. M. Kicken, N. F. A. Suos, M. P. J. Donners, C. J. den Reijer, A. J. Sandee, R. de Gelder, J. M. M. Smits, A. W. Gal, A. L. Spek, *Eur. J. Inorg. Chem.* **1999**, *9*, 1581–1592.
[43] C. Claver, E. Marco, L. A. Oro, M. Royo, E. Pastor, *Transition Met. Chem.* **1982**, *7*, 246.
[44] a) A. Sen, Z. Jiang, *Macromolecules* **1993**, *26*, 911–915; b) S. Stoccoro, G. Alesso, M. A. Cinellu, G. Minghetti, A. Zucca, A. Bastero, C. Claver, M. Manassero, *J. Organomet. Chem.* **2002**, *664*, 77–84.
[45] S. R. Bahr, P. J. Boudjouk, *J. Org. Chem.* **1992**, *57*, 5545–5547.
[46] M. Green, T. A. Kuc, S. H. Taylor, *J. Chem. Soc. A* **1971**, 2334.
[47] Collaborative Computational Project, Number 4. *Acta Crystallogr. Sect. D* **1994**, *50*, 760–763.
[48] G. M. Sheldrick, SHELX97, Program for crystal structure refinement, University of Göttingen, Germany, **1998**.
[49] L. J. Farrugia, *J. Appl. Crystallogr.* **1999**, *32*, 837–838.
[50] E. J. Baerends, D. E. Ellis, P. Ros, *Chem. Phys.* **1973**, *2*, 41–51.
[51] C. Fonseca Guerra, J. G. Snijders, G. te Velde, E. Baerends, *Theor. Chem. Acc.* **1998**, *99*, 391–403.
[52] G. T. Velde, E. J. Baerends, *J. Comput. Phys.* **1992**, *99*, 84–98.
[53] P. M. Boerrigter, G. T. Velde, E. J. Baerends, *Int. J. Quantum Chem.* **1988**, *33*, 87–113.
[54] L. Versluis, T. Ziegler, *J. Chem. Phys.* **1988**, *88*, 322–328.
[55] A. Becke, *Phys. Rev. A* **1988**, *38*, 3098–3100.
[56] a) J. P. Perdew, *Phys. Rev. B* **1986**, *34*, 7406; b) J. P. Perdew, *Phys. Rev. B* **1986**, *34*, 8822–8824.
[57] E. van Lenthe, A. E. Ehlers, E. J. Baerends, *J. Chem. Phys.* **1999**, *110*, 8943–8953, and references therein.
[58] F. Maseras, K. Morokuma, *J. Comput. Chem.* **1995**, *16*, 1170–1179.
[59] T. K. Woo, L. Cavallo, T. Ziegler, *Theor. Chem. Acc.* **1998**, *100*, 307–313.
[60] a) M. Clark, R. D. Cramer III, N. van Opdenbosch, *J. Comput. Chem.* **1989**, *10*, 982–1012; b) U. C. Singh, P. A. Kollman, *J. Comput. Chem.* **1986**, *7*, 718–730.
[61] A. K. Rappé, C. J. Casewit, K. S. Colwell, W. A. Goddard III, W. M. Shiff, *J. Am. Chem. Soc.* **1992**, *114*, 10024–10035.

Received: December 19, 2003
Revised: April 5, 2004
Published online: June 15, 2004

